BROWN-HET-444

A Study of Λ Parameters and Crossover Phenomena in SU(N) × SU(N) Sigma Models in Two Dimensions

by

J. Shigemitsu†

Physics Department, Brown University, Providence, RI 02912

and

J. B. Kogut*

Physics Department, University of Illinois, Urbana, IL 61801

†Supported in part by the Department of Energy under grant DE-AC02-76ER03130.A005 Task A-Theoretical.

*Supported in part by the NSF under grant NSF PHY79-00272.

Abstract

The spin system analogues of recent studies of the string tension and Λ parameters of SU(N) gauge theories in 4 dimensions are carried out for the SU(N) × SU(N) and O(N) models in 2 dimensions. The relations between the Λ parameters of both the Euclidean and Hamiltonian formulation of the lattice models and the Λ parameter of the continuum models are obtained. We calculate the one loop finite renormalization of the speed of light in the lattice Hamiltonian formulations of the O(N) and SU(N) × SU(N) models. Strong coupling calculations of the mass gaps of these spin models are done for all N and the constants of proportionality between the gap and the Λ parameter of the continuum models are obtained. These results are contrasted with similar calculations for the SU(N) gauge models in 3+1 dimensions. Identifying suitable coupling constants for discussing the $N \to \infty$ limits, our numerical results suggest that the crossover from weak to strong coupling in the lattice O(N) models becomes less abrupt as N increases while the crossover for the SU(N) × SU(N) models becomes more abrupt. The crossover in SU(N) gauge theories also becomes more abrupt with increasing N, however at an even greater rate than in the SU(N) × SU(N) spin models.

DISCLAIMER

1. Introduction

Considerable progress has been made recently towards understanding the dynamics of asymptotically free field theories. The lattice regulated versions of these models have been studied using Monte Carlo computer simulations[1], Monte Carlo renormalization groups[2,3], strong coupling expansions [4,5,6] etc. Many of the models have been shown to exist in a single phase for all coupling and estimates of a few physical quantities, such as correlation lengths, characterizing the continuum limits of the models have been made. Other approaches to the same physics have been made directly in the continuum formulations of the models. These include dilute instanton gas approximation[7] dense instanton calculations[8], loop space approaches[9], $N \rightarrow \infty$ limits[10], etc. These approaches may eventually expose the physics in the models more clearly than the lattice formulations and they may lead to some useful analytic results. However, to this date only the lattice approach can claim to have produced hard, numerical results.

Lattice approaches consist of several steps. Although different calculational schemes vary in their details, one typically must first compute the renormalization group trajectories of the theory's bare coupling constant. And, second, properties of the continuum limits of the lattice regulated theory are extracted and in some cases, compared with experiment. The first step in this program has shown that several of these models, asymptotically free spin systems in two dimensions and gauge theories in four dimensions, experience a sharp crossover phenomenon: at small coupling ordinary Feynman diagrams are adequate but as the coupling increases a point is reached where the renormalization properties of the theory abruptly change to those of the strong coupling limit. Although interesting in their own right, such results are of limited use because they refer to a particular lattice formulation of the model. The renormalization group trajectories are universal - independent of the regularization procedure - only near the critical point at zero coupling. The intermediate and strong coupling form of the trajectories depend on details such as the lattice approximation to the continuum derivative, the presence of irrelevant operators in the lattice action, the degree of asymmetry of the lattice itself, etc. For this reason, the second step in the program is actually more significant. Once the approach of the lattice theory to its renormalized continuum limit is mastered, relations between physical quantities independent of the lattice scaffolding can be found. It is these relations that allow one to compare different theories in a meaningful way.

To carry out the second step of the program one must set the scale of lattice calculations in terms of a physically meaningful scale of the continuum formulation of the theory. One such quantity which has been used in the context of gauge theories is the Λ parameter characterizing the scale of the weak coupling deviations from the free field behavior. The precise meaning of Λ will be discussed below. And once Λ is in hand, other mass scales of the continuum limit can be measured in terms of it. These include mass gaps (inverse correlation length) which must be calculated with non-perturbative methods and are therefore accessible to lattice analysis. The proportionality between mass and Λ is a pure number characterizing the continuum limit of the theory and it is useful to study it for various families of models. Calculations of Λ parameters and mass gaps for $SU(N) \times SU(N)$ and $O(N)$ spin systems in two dimensions and their comparisons to analogous calculations in $SU(N)$ gauge theories in four dimensions constitute the major portion of the present work.

One of our findings will be the following. The vector models and matrix models have different systematics as N varies. If we consider the ratios C_N=mass/Λ for each model, then it is observed that C_N decreases for the O(N) models as N increases, but increases for the matrix models. The analogue of C_N for the gauge models also increases as N increases at an even swifter rate than for the spin systems. These results and possible explanations for them have been presented recently in a short summary of the present rather lengthy analysis [11].

Our calculations of mass gaps and Λ parameters will be presented in considerable detail for the SU(N) x SU(N) spin systems. Discussion of the O(N) models will be briefer because they are considerably simpler. Results on the SU(N) gauge theories will be taken from other recent contributions in the literature.[5] However, we have included Appendices on SU(N) group theory so that the lattice calculations in the matrix models can be verified to the precision we have done them and so they could be extended by the interested reader.

The lattice action of the SU(N) x SU(N) spin systems is,

$$S = -\frac{1}{g^2}\sum_{x,\mu} \mathrm{tr}\left\{\left[U(x)U^{\dagger}(x+\mu) - 1\right] + \mathrm{h.c.}\right\} \tag{1.1}$$

The model has the global SU(N) x SU(N) symmetry because Eq. (1.1) is invariant under the transformation,

$$\begin{aligned} U(x) &\longrightarrow G_L U(x)\, G_R^{\dagger} \\ U^{\dagger}(x+\mu) &\longrightarrow (G_L U(x+\mu)\, G_R)^{\dagger} \end{aligned} \tag{1.2}$$

where G_L and G_R are two arbitrary members of the group SU(N). The O(N) models have the action

$$S = -\frac{1}{g}\sum_{x,\mu} \underset{\sim}{M}(x)\cdot\underset{\sim}{M}(x+\mu) \tag{1.3}$$

where $\underset{\sim}{M}(x)$ is an N- component unit vector. And finally, the action of SU(N) lattice gauge theory is,

$$S = -\frac{1}{g^2}\sum_{p} \mathrm{tr}\left\{\left[U(p)-1\right] + \mathrm{h.c.}\right\} \tag{1.4}$$

where $U(p)$ is the product of SU(N) matrices around the boundary of the plaquette p.

The first indication that the dynamics of the models Eq. (1.1) and (1.4) should be similar came from the Midgal recursion relation[12]. In this approximate scheme the coupling constant renormalization problem is identical in both models. A puzzling feature of this suggestion is that the gauge model has instantons for all N while the matrix spin systems do not. Since instantons are a natural disordering mechanism one might expect that this difference would appear in the renormalization group flows in the crossover region. We shall find that the systematics in the spin and gauge systems are similar, but the crossover phenomenon in the gauge systems is, in fact, more abrupt. This may be due to instantons but it may also be due simply to the higher space-time dimensionality or other disordering mechanisms such as vortices, etc. Another similarity between the two classes of models is the possible presence of a Gross-Witten[13] third order phase transition in their $N \to \infty$ limits[14]. This singularity may also be contributing to the sharp crossover found in these models at large but finite N. The recent suggestion that roughening[15] in the flux tube sector of the gauge model contributes to the rapid crossover phenomenon seems unlikely in view of several recent calculations. In Hamiltonian lattice gauge theory the on-axis flux tube roughens in the weak coupling region and not in the crossover region[16]. And recent Monte Carlo investigations of the specific heat of the SU(2) models show rapid crossover in the bulk thermodynamics of the model[17].

We have also carried out our calculations for the O(N) models because they have interesting properties. Their $N \to \infty$ limit is soluble and a well-defined $^1/N$ expansion exists for this family of models[18]. No solution is yet in hand for the $N \to \infty$ limit of the matrix models and it appears unlikely that a $^1/N$ expansion exists. In the context of our lattice calculations, we shall find singularities of the deWit - 't Hooft type[19] which indicate that the analyticity needed for a $^1/N$ expansion does not appear to exist here. Of course, such singularities do not exist for the O(N) models. We will compare our numerical results with Monte Carlo renormalization group studies of the O(3) model and the exact solution for the $N \to \infty$ limit and find good agreement. It is amusing that the O(3) model has the most abrupt crossover region in this class of models and only it has instantons.

Now lets introduce the idea of the Λ parameters since they play a central role in our calculations. A convenient way to compare two definitions of coupling constants in the weak coupling limit is in terms of the Λ parameters. For bare coupling constants these parameters appear as follows. Consider the two loop Callan-Symanzik function for the continuum models.

$$M \frac{\partial f}{\partial M} = \beta(f) = -\beta_o f^2 - \beta_1 f^3 \tag{1.5}$$

where,

M = Pauli Villars cutoff mass

f = bare coupling constant

For the O(N) models one should let

$$f \longrightarrow \bar{g} \equiv (N-2)\, g \tag{1.6}$$

and[20]

$$\beta(\bar{g}) = -\frac{1}{2\pi} \bar{g}^2 - \frac{1}{4\pi^2 (N-2)} \bar{g}^3 \tag{1.7}$$

For the Chiral models one has [21]

$$f \longrightarrow \lambda = Ng^2 \tag{1.8}$$

$$\beta(\lambda) = -\frac{1}{8\pi}\lambda^2 - \frac{1}{128\pi^2} \lambda^3 \tag{1.9}$$

To integrate eq.(1.5) the scale of the cutoff mass M must be set. This is done by introducing a mass parameter Λ,

$$\frac{\partial f}{\partial \ln M/\Lambda} = -\beta_o f^2 - \beta_1 f^3 - \ldots \tag{1.10}$$

Integrating eq. (1.10) and choosing the integration constant appropriately one obtains the two loop result,

$$f(M) = \frac{1}{\beta_o \ln \frac{M}{\Lambda} + \frac{\beta_1}{\beta_o} \ln(\ln\frac{M}{\Lambda})} \tag{1.11}$$

The particular choice for the integration constant in eq. (1.11) has the virtue that the two loop contribution does not add a constant to the denominator of eq. (1.11) and so does not affect the coupling constant used in the one loop approximation. With this convention the Λ parameter, the bare coupling f and the cutoff mass M are related by

$$\Lambda = M\,(\beta_o f)^{-\beta_1/\beta_o^2} \exp\left(-\frac{1}{\beta_o f}\right)\left[1-0(f)\right] \tag{1.12}$$

Note that for $\frac{M}{\Lambda} >> 1$ it is perfectly adequate to replace (1.11) by,

$$f(M) \cong \frac{1}{\beta_o \ln\frac{M}{\Lambda}} \tag{1.13}$$

The same procedures that took us from eq. (1.5) to (1.13) can also be carried out for the lattice regularized theory and one introduces in this way a lattice Λ_L . The cutoff mass M is replaced by the lattice cutoff $^1/a$ and instead of $f(M)$ one has the bare lattice coupling constant $f_L(a)$. Also eq. (1.12) is replaced by (recall that β_o and β_1 are universal constants independent of regularization scheme)

$$\Lambda_L = \frac{1}{a}\left(\beta_o f_L\right)^{-\beta_1/\beta_o^2} \exp\left(-\frac{1}{\beta_o f_L}\right)\left[1+0(f_L)\right] \tag{1.14}$$

In the limit $\frac{1}{a\Lambda_L} >> 1$ one has again in analogy to eq. (1.13)

$$f_L(a) \cong \frac{1}{\beta_o \ln\frac{1}{a\Lambda_L}} \tag{1.15}$$

The relation between Λ and Λ_L is fixed by requiring that the renormalized theories give the same physics independent of the regularization scheme. The renormalized continuum theory is written in terms of the

renormalized coupling f_R

$$\frac{1}{f_R} = \frac{z_1}{f} \equiv \frac{1}{f} + B(M) \tag{1.16}$$

where we have written, $z_1 = 1 + B(M)f$

Similarly for the renormalized lattice theory one has,

$$\frac{1}{f_R^L} = \frac{z_{1L}}{f_L(a)} = \frac{1}{f_L(a)} + B_L(a) \tag{1.17}$$

Regularization scheme independence requires

$$\frac{z_1}{f_{(M)}} = \frac{z_{1L}}{f_{L}(a)}$$

or

$$\frac{1}{f_{L}(a)} - \frac{1}{f_{(M)}} = B(M) - B_L(a) \tag{1.18}$$

Inserting (1.13) and (1.15),

$$\frac{\Lambda}{\Lambda_L} = aM \exp\left[\frac{1}{\beta_o}\Big(B(M) - B_L(a)\Big)\right] \tag{1.19}$$

In the next two sections we will calculate $B(M) - B_L(a)$ through one loop and hence also $^\Lambda/_{\Lambda_L}$. We consider both a Euclidean as well as a spatial lattice regularization scheme. The importance of the number $^\Lambda/_{\Lambda_L}$ becomes clear when one recalls that physical masses, being renormalization group invariants, obey relations such as eq. (1.12) and eq. (1.14) the only difference being that there are proportionality constants C and C_L on the R.H.S. of the two respective equations. In other words

$$\text{Mass} = C\Lambda = C_L\Lambda_L \tag{1.20}$$

The constant C cannot be obtained within the framework of ordinary continuum weak coupling perturbation theory. The lattice setup, however, also lends itself to "non-perturbative" analyses (e.g. strong coupling or Monte Carlo) and one can estimate C_L. Once C_L is known the quantity of interest, the C of the continuum theory, can be obtained from eq. (1.20) and previous calculations of Λ/Λ_L.

The rest of this article is organized as follows. Section 2 discusses Λ/Λ_E, where "E" stands for "Euclidean lattice regularization". For the $SU(N)\otimes SU(N)$ Chiral models we use the Background Field method[22]. This method was adapted recently in ref. (23) to lattice theories involving matrix degrees of freedom. For the O(N) models Λ/Λ_E has been calculated previously by G. Parisi[24]. Section 3 presents calculations of Λ/Λ_H, where "H" denotes "spatial lattice regularization". Since our mass gap calculations are carried out within a Hamiltonian framework it is this ratio Λ/Λ_H that will be required to relate the physical mass to the Λ parameter of the continuum theory. Section 4 discusses the mass gap calculations themselves. We use the results of this section both to obtain the values for the "C" 's as well as to investigate the crossover from strong to weak coupling behavior in the spin models. Finally all our 2D results are compared with previous calculations[5] on SU(N) gauge theories in 4D.

2. Regularization of SU(N) x SU(N) Chiral Models. The Background Field Technique.

The background field regularization method has proven to be an efficient and clear technique for carrying out the one loop, perturbative renormalization program for many continuum field theories. It has been applied to SU(N) lattice gauge theory in 3 + 1 dimensions[23] and quantitative relationships to continuum renormalization procedures obtained by more straight-forward tedious methods have been rederived.[25] In this section we shall apply the method to the continuum and lattice versions of the SU(N) chiral spin systems in two Euclidean dimensions. The analogous calculations for the lattice Hamiltonian model will be presented in the next section.

Our calculations will follow those of Ref. (23) quite closely. We begin with the lattice action of Eq. (1.1)

$$S = -\frac{1}{g^2}\sum_{x,\mu} \mathrm{tr}\left[\left(U(x)U^\dagger(x+\mu) - 1\right) + \text{h.c.}\right] \tag{2.1}$$

The partition function is given by

$$Z = \int \prod_x dU\, e^{-S} \tag{2.2}$$

and dU = invariant Haar measure over the group SU(N).

Since we are going to apply ordinary perturbation theory here, we want to separate the fluctuations of the $U(x)$ into two parts: "low frequency" fluctuations whose dynamics are renormalized when the "high frequency" fluctuations are integrated out of the partition function Eq. (2.2). This physical idea -- the basis of all renormalization programs -- is nicely implemented by the background field method. Write,

$$U(x) = e^{ig\phi(x)}U^{cl}(x) \tag{2.3}$$

where $U^{cl}(x)$ solves the classical equations of motion of the lattice theory and $\phi(x)$ parametrizes the quantum fluctuations of $U(x)$. It is convenient to define

$$\phi(x) = \lambda^{\alpha}\phi^{\alpha}(x) \quad , \quad \alpha = 1,2,\ldots, N^2 - 1 \tag{2.4}$$

where the λ^{α} matrices provide a representation of the Lie Algebra

$$[\lambda^{\alpha},\lambda^{\beta}] = if^{\alpha\beta\gamma}\lambda^{\gamma} \tag{2.5}$$

with the normalization condition

$$tr(\lambda^{\alpha}\lambda^{\beta}) = \frac{1}{2}\,\delta^{\alpha\beta} \quad . \tag{2.6}$$

Substituting Eq. (2.3) into (2.1) gives

$$\begin{aligned} S = &- \frac{1}{g^2}\sum_{x,\mu} tr\left[\left(U^{cl}(x)U^{cl^{\dagger}}(x+\mu) - 1\right) + h.c.\right] \\ &- \frac{1}{g^2}\sum_{x,\mu} tr\left[\left(e^{-ig\phi(x+\mu)}e^{ig\phi(x)} - 1\right)U^{cl}(x)U^{cl^{\dagger}}(x+\mu) + h.c.\right] \end{aligned} \tag{2.7}$$

where the terms have been organized in a convenient fashion. The exponentials in Eq. (2.7) can be expanded in powers of g,

$$\begin{aligned} e^{-ig\phi(x+\mu)}e^{ig\phi(x)} &= \exp[-ig\nabla_{\mu}\phi(x) + \frac{1}{2}\,g^2[\phi(x+\mu),\phi(x)] + O(g^3)] \\ &= 1 - ig\nabla_{\mu}\phi(x) + \frac{1}{2}\,g^2[\phi(x+\mu),\phi(x)] - \frac{1}{2}\,g^2(\nabla_{\mu}\phi(x))^2 + O(g^3) \end{aligned} \tag{2.8}$$

where ∇_{μ} denotes the discrete lattice difference. Similarly, the integration measure should be expanded,

$$dU = \prod_{\alpha=1}^{N^2-1} d\phi^{\alpha}[1 + O(g^2\phi^2)] \tag{2.9}$$

The $O(g^2\phi^2)$ correction to the measure does not affect one loop calculations and can be ignored. This fact constitutes one of several advantages the background method has over other renormalization methods. Next, it is convenient to parametrize $U^{cl}(x)U^{cl^{\dagger}}(x+\mu)$ appearing in Eq. (2.7) as

$$U^{cl}(x)U^{cl^{\dagger}}(x+\mu) = \exp(iF_{\mu}(x)) \tag{2.10}$$

where F_{μ} is a hermitian matrix

$$F_{\mu}(x) = \lambda^{\alpha}F^{\alpha}_{\mu}(x) \tag{2.11}$$

Expanding Eq. (2.10) in powers of $F_{\mu}(x)$ and substituting the result along with Eq. (2.7) into Eq. (2.8) we have,

$$\begin{aligned} S = &- \frac{1}{g^2}\sum_{x,\mu} trF_{\mu}F_{\mu} - \sum_{x,\mu} tr\Big\{-\frac{1}{2}\,(\nabla_{\mu}\phi)^2(2 - F^2_{\mu}) \\ &+ i[\phi(x+\mu),\phi(x)]F_{\mu}\Big\} + O(g^2,F^4) \end{aligned} \tag{2.12}$$

And, finally, using Eq. (2.4) and (2.11) we can write S as the sum of three pieces appropriate for perturbation theory

$$S = S^{cl} + S_o + S_{int} + O(g^2, F^4) \tag{2.13a}$$

where

$$S^{cl} = -\frac{1}{2g^2} \sum_{x,\mu} (F_\mu^\alpha)^2 \quad , \tag{2.13b}$$

$$S_o = \sum_{x,\mu} \frac{1}{2} (\nabla_\mu \phi^\alpha)^2 \tag{2.13c}$$

and

$$\begin{aligned} S_{int} = \sum_{x,\mu} \Big\{ & -\frac{1}{2} \mathrm{tr}(\lambda^\alpha \lambda^\beta \lambda^\gamma \lambda^\delta) \nabla_\mu \phi^\alpha \nabla_\mu \phi^\beta F_\mu^\gamma F_\mu^\delta \\ & + \frac{1}{2} f^{\alpha\beta\gamma} \phi^\alpha (x+\mu) \phi^\beta (x) F_\mu^\gamma \Big\} \end{aligned} \tag{2.13d}$$

It will also prove convenient to give the fields ϕ^α a small mass m so that all the integrals encountered in the perturbation calculations are infrared finite

$$S_o \longrightarrow \sum_{x,\mu} \left[\frac{1}{2} (\nabla_\mu \phi^\alpha)^2 + \frac{1}{2} m^2 \phi^{\alpha 2} \right] \tag{2.14}$$

We shall see that all the physical quantities of interest to us are actually infrared finite and the limit $m \to 0$ will be taken at the end of our calculations. However, to avoid possible ambiguities in intermediate steps the modification Eq. (2.14) will be employed. More importantly, the perturbation theory calculations will also require renormalization. The square lattice will provide the cutoff in the formulation Eq. (2.13). This regularization

procedure will be compared with the continuum Pauli-Villars method which we will discuss now. The continuum form of Eq. (2.13) is quite clear. The lattice difference operator becomes the differential ∂_μ and Eq. (2.13d) simplifies to

$$S_{int}^{cont} = \frac{1}{2} f^{\alpha\beta\gamma} \int \partial_\mu \phi^\alpha \phi^\beta \mathcal{F}_\mu^\gamma d^2x \tag{2.15a}$$

where

$$\mathcal{F}_\mu^\gamma(x) = F_\mu^\gamma(x)/a \tag{2.15b}$$

and "a" is the Euclidean lattice spacing. It is clear from Eq. (2.10) that $F_\mu^\gamma(x)$ is proportional to a, so $\mathcal{F}_\mu^\gamma(x)$ has a finite continuum limit. Note also that the first term of Eq. (2.13c) vanishes in the continuum model since it becomes proportional to the lattice spacing a itself.

Now we can easily perform the one loop renormalization on the continuum partition function. From Eq. (2.13) and (2.15),

$$\begin{aligned} Z &= \int \Pi d\phi^\alpha e^{-S^{cl} - S_o - S_{int}} [1 + O(g^2, F^4)] \\ &= e^{-S^{cl}} \int \Pi d\phi^\alpha e^{-S_o} \left\{ 1 - S_{int} + \frac{1}{2} S_{int}^2 + - \ldots \right\} \\ &= e^{-S^{cl}} \left\{ 1 - \langle S_{int} \rangle + \frac{1}{2} \langle S_{int}^2 \rangle + \ldots \right\} \end{aligned} \tag{2.16}$$

The term $\langle S_{int} \rangle$ vanishes identically because of the gradient in Eq. (2.15a). The next term can be evaluated

$$\begin{aligned} \frac{1}{2} \langle S_{int}^2 \rangle &= \frac{1}{8} \int d^2y \, d^2y' \, f^{\alpha\beta\gamma} f^{\alpha'\beta'\gamma'} \mathcal{F}_\mu^\gamma(y) \mathcal{F}_\nu^{\gamma'}(y') \langle \partial_\mu \phi^\alpha(y) \phi^\beta(y) \partial_\nu \phi^{\alpha'}(y') \phi^{\beta'}(y') \rangle \\ &= \frac{N}{8} \int d^2y \, d^2y' \mathcal{F}_\mu^\gamma(y) \mathcal{F}_\nu^\gamma(y') \left[G(y-y') \partial_\mu \partial_\nu' G(y-y') - \partial_\mu G(y-y') \partial_\nu' G(y-y') \right] \end{aligned} \tag{2.17}$$

where we have used the identity $f^{\alpha\rho\gamma}f^{\alpha\rho\gamma'} = N\delta_{\gamma\gamma'}$, and G is a scalar propagator of the free action S_o of Eq. (2.14),

$$G(y) = \int \frac{d^2k}{(2\pi)^2}\frac{e^{ik\cdot y}}{k^2+m^2} \equiv \int \frac{d^2k}{(2\pi)^2}\frac{e^{ik\cdot y}}{D(k)} . \tag{2.18}$$

The two terms of Eq. (2.17) can be combined if we integrate by parts and use the requirement that the background field $\mathcal{F}$ be slowly varying,

$$\partial_\mu \mathcal{F}_\nu << \mathcal{F}_\nu \quad , \tag{2.19}$$

then

$$\frac{1}{2}<S^2_{int}> = \frac{N}{4}\int d^2y d^2y' \mathcal{F}^\gamma_\mu(y)\mathcal{F}^\gamma_\nu(y')G(y-y')(-\partial_\mu\partial_\nu)G(y-y') . \tag{2.20}$$

Now the spatial variation of $\mathcal{F}$ is negligible compared to that of the Green's functions in Eq. (2.20). Therefore $\mathcal{F}^\gamma_\mu(y)$ can be replaced by $\mathcal{F}^\gamma_\mu(y')$ and the y-integration performed over the Green's functions. Then only the terms in the μ and ν sums with $\mu=\nu$ contribute to the integral and Eq. (2.20) becomes

$$\begin{aligned}\frac{1}{2}<S^2_{int}> &= \frac{N}{4}\int d^2y' \mathcal{F}^\gamma_\mu(y')\mathcal{F}^\gamma_\nu(y')\int d^2y G(y-y')(-\tfrac{1}{2}\delta_{\mu\nu}\cdot\partial^2_\lambda)G(y-y')\\ &= \frac{N}{4}\int d^2y'\,\frac{1}{2}\left(\mathcal{F}^\gamma_\mu(y')\right)^2\int d^2y G(y-y')\delta^2(y-y')\\ &= \frac{N}{4}G(0)\int d^2y\,\frac{1}{2}\left(\mathcal{F}_\mu(y)\right)^2\\ &= \frac{N}{4}G(0)\cdot S^{cl} .\end{aligned} \tag{2.21}$$

Finally, substituting back into Eq. (2.16) and exponentiating,

$$\begin{aligned}Z &= e^{-\left[\frac{1}{g^2}-\frac{N}{4}G(0)\right]\frac{1}{2}\int d^2y \mathcal{F}^\gamma_\mu\mathcal{F}^\gamma_\mu}\\ &\equiv e^{-\frac{z_1}{g^2}S^{cl}} .\end{aligned} \tag{2.22}$$

where the coupling constant renormalization Z_1 is identified

$$z_1 = 1 - \frac{g^2}{4}N\,G(0) \tag{2.23}$$

Eq. (2.23) is a formal expression until we specify the continuum regularized definition of $G(0)$. If the Pauli-Villars scheme is used, then the usual analysis shows that $G(0)$ is replaced by

$$G^{P.V.}(0) = \int\frac{d^2k}{(2\pi)^2}\left\{\frac{1}{k^2+m^2} - \frac{1}{k^2+M^2}\right\} \tag{2.24}$$

where M is the regulator mass. Then Eq. (2.23) becomes

$$\begin{aligned}z_1 &= 1 - \frac{Ng^2}{4}G^{P.V.}(0)\\ &= 1 - \frac{Ng^2}{8\pi}\ln(M/m)\end{aligned} \tag{2.25}$$

Eq. (2.25) contains some interesting physics. The minus sign is characteristic of asymptotic freedom. It is clear from Eq. (2.23) that the renormalized coupling constant is

$$g^2_R = g^2/z_1 = g^2 + \frac{Ng^4}{8\pi}\ln(M/m) + \ldots \tag{2.26}$$

Thus integrating out the "high frequency" fluctuations has increased the coupling between the "low frequency" components of the field. Describing this in terms of a Callan-Symanzik β function, we can require that g_R be fixed as the ultraviolet cutoff M is varied

$$M \frac{\partial}{\partial M} g_R^2 = 0 = M \frac{\partial}{\partial M} g^2 + \frac{Ng^4}{8\pi} + \text{higher orders} \tag{2.27}$$

So

$$M \frac{\partial}{\partial M} g^2 \equiv \beta(g^2) = - \frac{N}{8\pi} g^4 + \ldots \tag{2.28}$$

which agrees with the conventional result to this order. We have chosen to write the renormalization group trajectory in terms of the bare coupling and the ultraviolet cutoff rather than the renormalized coupling and a subtraction momentum. This calculation also illustrates some of the better features of the background field method -- it led us directly to the coupling constant renormalization constant without any additional wave function renormalization calculations needed.

Now we turn to the Euclidean lattice calculation using Eq. (2.13). We must again compute the terms in Eq. (2.16). The first is

$$\begin{aligned} \langle S_{int} \rangle = \sum_{x,\mu} - \frac{1}{2} \Big\{ & \mathrm{tr}(\lambda^\alpha \lambda^\beta \lambda^\gamma \lambda^\delta) F_\mu^\gamma F_\mu^\delta \langle \nabla_\mu \phi^\alpha \nabla_\mu \phi^\beta \rangle \\ & + \frac{1}{2} f^{\alpha\beta\gamma} F_\mu^\gamma \langle \phi^\alpha (x + \mu) \phi^\beta (x) \rangle \Big\} \end{aligned} \tag{2.29}$$

The second term in Eq. (2.29) vanishes identically since it is the average value of a vector quantity. The SU(N) indices of the first term can be simplified by using the identity

$$\mathrm{tr}\lambda^\alpha \lambda^\beta \lambda^\gamma \lambda^\delta = \frac{1}{8} \left(\frac{2}{N} \delta^{\alpha\beta} \delta^{\gamma\delta} - f^{\alpha\beta a} f^{\gamma\delta a} + d^{\alpha\beta a} d^{\gamma\delta a} - i f^{\alpha\beta a} d^{\gamma\delta a} - i d^{\alpha\beta a} f^{\gamma\delta a} \right) \tag{2.30}$$

Only the first term of Eq. (2.30) contributes to Eq. (2.29) when α and β are contracted, as one can easily show using the tracelessness of the $f^{\alpha\beta\gamma}$ and the $d^{\alpha\beta\gamma}$ symbols. Now

$$\begin{aligned} \langle S_{int} \rangle &= - \frac{1}{8N} \sum_x \frac{1}{2} (F_\nu^\gamma)^2 \langle (\nabla_\mu \phi^\alpha)^2 \rangle \\ &= - \frac{1}{8N} \sum_x \frac{1}{2} (F_\nu^\gamma)^2 \, 4(N^2 - 1) \big(G(0) - G(1) \big) \end{aligned} \tag{2.31}$$

where G denotes a lattice propagator

$$G(x) = \langle \phi^1(x) \phi^1(0) \rangle = \int_{-\pi}^{\pi} \frac{d^2 k}{(2\pi)^2} \frac{e^{ik \cdot x}}{4 - 2\cos k_1 - 2\cos k_1 + m^2 a^2} . \tag{2.32}$$

Using the amusing identity

$$G(1) - G(0) = - \frac{1}{4} + O(m^2 a^2) \tag{2.33}$$

which can easily be checked, Eq. (2.31) becomes

$$\langle S_{int} \rangle = \frac{N^2 - 1}{8N} \sum_x \frac{1}{2} (F_\nu^\gamma)^2 = \frac{1}{4} C_N \cdot S^{cl} \tag{2.34}$$

where we have identified the classical lattice action and the quadratic Casimir of the fundamental representation $C_N = (N^2 - 1)/2N$.

The last term in Eq. (2.16) requires more care,

$$\frac{1}{2}\langle S^2_{int}\rangle = \frac{1}{8} f^{\alpha\beta\gamma}f^{\alpha'\beta'\gamma'} \sum_{y,y',\mu,\nu} F^{\gamma}_{\mu}(y)F^{\gamma'}_{\nu}(y')\langle\phi^{\alpha}(y+\mu)\phi^{\beta}(y)\phi^{\alpha'}(y'+\nu)\phi^{\beta'}(y')\rangle + O(F^4)$$

$$= \frac{N}{8}\sum_{y,y',\mu,\nu} F^{\gamma}_{\mu}(y)F^{\gamma}_{\nu}(y')\Big[G(y-y'+\mu-\nu)G(y-y') - G(y-y'+\mu)\,G(y-y'-\nu)\Big] \tag{2.35}$$

where we used the identity $f^{\alpha\beta\gamma}f^{\alpha\beta\gamma'} = N\delta_{\gamma\gamma'}$. It is convenient to write the propagators in momentum space using Eq. (2.32). Define

$$\Delta(k) = 4 - 2\cos k_1 - 2\cos k_2 + m^2a^2 \tag{2.36}$$

so

$$\frac{1}{2}\langle S^2_{int}\rangle = \frac{N}{8}\sum F^{\gamma}_{\mu}(y)F^{\gamma}_{\nu}(y')\int\frac{d^2k}{(2\pi)^2}\frac{d^2k'}{(2\pi)^2}\frac{e^{ik_\mu}\left(e^{-ik_\nu}-e^{-ik'_\nu}\right)e^{ik(y-y')}e^{ik'(y-y')}}{\Delta(k)\Delta(k')} \tag{2.37}$$

The background field $F^{\gamma}_{\nu}(y')$ is slowly varying, so the y' summation can be done by simply ignoring its spatial variation

$$\frac{1}{2}\langle S^2_{int}\rangle = \frac{N}{8}\sum_{y,\mu,\nu} F^{\gamma}_{\mu}(y)F^{\gamma}_{\nu}(y)\int\frac{d^2k}{(2\pi)^2}\frac{e^{ik_\mu}\left(e^{-ik_\nu}-e^{ik_\nu}\right)}{\Delta^2(k)} \tag{2.38}$$

The momentum integral vanishes unless $\mu = \nu$, so

$$\frac{1}{2}\langle S^2_{int}\rangle = \frac{N}{4}\cdot S^{cl}\cdot\int\frac{d^2k}{(2\pi)^2}\frac{e^{ik_1}\left(e^{-ik_1}-e^{ik_1}\right)}{\Delta^2(k)} \tag{2.39}$$

The momentum integral here is, in fact, a disguised form of $G(1)$. We show this and discuss other relevant properties of lattice propagators in Appendix A. Granting this, Eq. (2.39) becomes

$$\frac{1}{2}\langle S^2_{int}\rangle = \frac{N}{4}\cdot G(1)\cdot S^{cl} \tag{2.40}$$

Collecting Eq. (2.16), (2.34) and (2.40), we have the partition function with the fluctuations integrated out

$$Z = \exp\left[-\frac{z_1^L}{g^2}\sum_x \frac{1}{2}(F^{\gamma}_{\mu})^2\right] \tag{2.41}$$

with

$$z_1^L = 1 - g^2\left(\frac{N}{4}G^L(1) + \frac{1}{4}C_N\right) = 1 - g^2\left(\frac{N}{4}G^L(0) + \frac{C_N}{4} - \frac{N}{16}\right) \tag{2.42}$$

where the superscript L reminds us that these are lattice quantities. It is clear that we can infer that the lattice theory is asymptotically free and obtain the Callan Symanzik function as in Eq. (2.28). Now, however, g refers to the bare coupling on the lattice of spacing "a" which replaces the inverse of the Pauli-Villars regulator mass M.

Now we wish to go beyond the β functions and relate the length scales of the continuum and lattice models as well. This is done along the lines discussed in the introduction. Λ_E and $\Lambda_{P.V.}$ are introduced and the requirement that the long distance physics be the same in both descriptions fixes their ratio according to Eq. (1.19). Using (2.25) and (2.42) one obtains

$$\frac{\Lambda^{P.V.}}{\Lambda_E} = \sqrt{32}\, e^{\pi(N^2-2)/2N^2} \tag{2.43}$$

and a large change of scale is observed. For comparison, we write down the analogous Λ-ratio for the $O(N)$ vector models

$$\left(\frac{\Lambda^{P.V.}}{\Lambda_E}\right)_{O(N)} = \sqrt{32}\, e^{\frac{\pi}{2(N-2)}} \tag{2.44}$$

Note that the O(4) result and the SU(2) x SU(2) calculation agree as they must. One also notices that the exponential factor in Eq. (2.43) has a finite non-trivial $N \to \infty$ limit in distinction to the O(N) model.

$$\frac{\Lambda^{P.V.}}{\Lambda_E} \xrightarrow[N \to \infty]{} e^{\pi/2} \cdot \sqrt{32} = (4.81047 \;\ldots)\sqrt{32} \qquad (2.45)$$

The matrix vs. the vector character of the two models must be the reason behind these different limiting features.

3. Spatial Lattice Regularization

In this section we discuss the relationship between coupling constants in the Hamiltonian and the Euclidean versions of the theory.

First, recall that the Hamiltonian is obtained from the partition function of the Euclidean lattice by letting the timelike lattice spacing a_t tend to zero in the transfer matrix. This corresponds to introducing couplings K_t and K_s for timelike and spacelike links and then taking a very anisotropic limit.

So, we begin with the action,

$$S = -\sum_{\text{sites}} \left\{ K_t \,\mathrm{tr}\left(U(r)U^\dagger(r+\hat{e}_t) + \text{h.c.}\right) + K_s \,\mathrm{tr}\left(U(r)U^\dagger(r+\hat{e}_s) + \text{h.c.}\right)\right\} \qquad (3.1)$$

where $\hat{e}_t(\hat{e}_s)$ is a unit lattice vector in the time (space) direction. Standard methods reveal the transfer matrix,

$$\hat{T} = \exp\left\{-\frac{1}{2K_t}\sum_{\ell} \hat{\underset{\sim}{E}}^2(\ell) + K_s \sum_{\ell} \mathrm{tr}\left(\hat{U}(\ell)\hat{U}^\dagger(\ell+1) + \text{h.c.}\right)\right\} \qquad (3.2)$$

where

$\sum_{\ell}$ = sum over all sites in a given time slice

$\hat{E}^\alpha$ = α^{th} generator of left SU(N) rotations (right SU(N) rotations could have been used equally well)

$\hat{\underset{\sim}{E}}^2 = \sum_{\alpha=1}^{N^2-1} \hat{E}^{\alpha^2}$ = quadratic Casimir operator of SU(N)

Furthermore, we are working in a space of state $\prod_{\text{links}} |U\rangle$ diagonal in U.

$$\begin{aligned} \hat{U}^\nu_{\alpha\beta}\,|U\rangle &= U^{(\nu)}_{\alpha\beta}\,|U\rangle \\ \left[\hat{E}^\alpha, \hat{U}\right] &= -\frac{1}{2}\lambda^\alpha \hat{U} \end{aligned} \qquad (3.3)$$

"ν" labels representations of SU(N) and we omit this superscript when we are using the fundamental representation.

Next we require that $\hat{T} \sim 1 - a_t\hat{H} + O(a_t^2)$ as a_t is taken to zero. Inspecting Eq. (3.2), we see that both $1/K_t$ and K_s should be proportional to a_t to insure this. Therefore, it is convenient to define,

$$\frac{1}{K_t} = \frac{a_t}{a} g_t^2 \quad , \quad K_s = \frac{a_t}{a} \frac{1}{g_s^2} \tag{3.4}$$

Note that when $a_t = a$ these definitions of g_t^2 and g_s^2 match onto the usual convention $K = 1/g^2$. However, letting $a_t \to 0$ in Eq. (3.2) and (3.4), we obtain the Hamiltonian,

$$\hat{H} = \frac{g_t^2}{2a} \sum_{\ell} \left\{ \hat{\underline{E}}^2(\ell) - \frac{2}{g_H^4}\left(\mathrm{tr}\ \hat{U}(\ell)\hat{U}^{\dagger}(\ell+1) + \mathrm{h.c.}\right)\right\} \tag{3.5}$$

where

$$g_H^2 = \sqrt{g_s^2\, g_t^2} \tag{3.6}$$

It is important to note the presence of two coupling constants in the lattice Hamiltonian — one (g_t^2) setting the scale of electric (static) effects and another (g_s^2) governing magnetic (kinetic) effects.

In the remainder of this section, we shall relate g_t^2 and g_H^2 to the coupling constant g^2 used in a continuum, Pauli-Villars regulated version of the theory in the limit that all g^2's are small. Only a slight modification of the background field method described in section 2 will be needed. Going through the same steps that led to Eqs. (2.13) and using the definitions Eq. (3.4) for g_t^2 and g_s^2 one finds that the action Eq. (3.1) is the sum of two pieces,

$$S = S^H_{cl.} + S^H_{eff} \tag{3.7}$$

where

$$S^H_{cl.} = a\sum_{\ell}\int dt \left\{ \frac{1}{2g_t^2}(\underline{F}_t)^2 + \frac{1}{2g_s^2}(\tfrac{1}{a}\underline{F}_z)^2 \right\} \tag{3.8}$$

and

$$S^H_{eff.} = a\sum_{\ell}\int dt \left\{ \frac{1}{2}(\partial_t\underline{\phi})^2 + \frac{1}{2}\eta(\tfrac{1}{a}\nabla\underline{\phi})^2 - \frac{1}{8N}\eta(\tfrac{1}{a}\nabla\underline{\phi})^2(\underline{F}_z)^2 \right.$$
$$\left. + \frac{1}{2} f^{\alpha\beta\gamma}\left[(\partial_t\phi^{\alpha})\phi^{\beta}F_t^{\gamma} + \frac{1}{a}\eta\phi^{\alpha}(\underline{r}+\hat{e}_s)\phi^{\beta}(\underline{r})(\tfrac{1}{a}F_z^{\alpha})\right]\right\} \tag{3.9}$$

In these equations we have made the substitutions,

$$a_t \sum \to \int dt$$
$$\frac{1}{a_t}\nabla_t \to \partial_t \tag{3.10}$$
$$\frac{1}{a_t}F_t^{\alpha} \to F_t^{\alpha} \qquad \text{(a different notation was used in section 2, where } \tfrac{1}{a}F_\nu \to \mathcal{F}_\nu)$$

appropriate to the $a_t \to 0$ limit and have also introduced the parameter,

$$\eta \equiv \frac{g_t^2}{g_s^2} \tag{3.11}$$

The free piece of S^H_{eff} is

$$S^H_o = a\sum\int dt \left\{ \frac{1}{2}(\partial_t\underline{\phi})^2 + \frac{1}{2}\eta(\tfrac{1}{a}\nabla\underline{\phi})^2 \right\} \tag{3.12}$$

which leads to a free propagator of the form,

$$G_H(\underline{r}) = \int \frac{d^2k}{(2\pi)^2}\frac{e^{ik_ot}e^{ikz}}{D_H(k)}$$
$$= \int_{-\infty}^{\infty}\frac{dk_o}{2\pi}\int_{-\pi/a}^{\pi/a}\frac{dk}{2\pi}\frac{e^{ik_ot}e^{ikz}}{[k_o^2 + \frac{\eta}{a^2}(2-2\cos ka)+m^2]} \tag{3.13}$$

As in the Euclidean calculation we must introduce an infrared regulator mass m^2 in our formulas and check that the limit $m^2 \to 0$ is smooth when one calculates quantities of physical significance.

The last two terms in S^H_{eff} constitute S^H_{int} and we must now calculate as in the Euclidean analysis,

$$\langle e^{-S^H_{eff}} \rangle = 1 - \langle S^H_{int} \rangle_o + \frac{1}{2} \langle S^{H^2}_{int} \rangle_o + O(g^2, F^2) \tag{3.14}$$

One obtains

$$-\langle S^H_{int} \rangle_o = \frac{N^2-1}{2N} \cdot \eta \left(G_H(0) - G_H(1) \right) \int_y \frac{1}{2} \left(\frac{1}{a} F_z \right)^2 \tag{3.15}$$

where we use the notation,

$$\int_y \equiv a \sum_\ell \int dy_o \tag{3.16}$$

and

$$\frac{1}{2} \langle S^{H^2}_{int} \rangle_o = \left(\frac{N}{2} \int \frac{d^2k}{(2\pi)^2} \frac{k_o^2}{D_H^2(k)} \right) \int_y \frac{1}{2} F_t^2$$

$$+ \left(\frac{N}{4} \frac{\eta^2}{a^2} \int \frac{d^2k}{(2\pi)^2} \frac{1-e^{2ika}}{D_H^2(k)} \right) \int_y \frac{1}{2} \left(\frac{1}{a} F_z \right)^2 \tag{3.17}$$

Manipulations similar to those employed on the Euclidean calculation enable us to identify the momentum integrals in Eq. (3.17) as $G_H(0)$ and $G_H(1)$,

$$\frac{N}{2} \int \frac{d^2k}{(2\pi)^2} \frac{k_o^2}{D_H^2(k)} = \frac{N}{4} G_H(0) \tag{3.18}$$

and,

$$\frac{N}{4} \cdot \frac{\eta^2}{a^2} \cdot \int \frac{d^2k}{(2\pi)^2} \frac{1-e^{2ika}}{D_H^2(k)} = \frac{N}{4} \cdot \eta \cdot G_H(1) \tag{3.19}$$

Collecting these results and substituting in Eq. (3.14) we have,

$$\langle e^{-S^H_{eff}} \rangle = 1 + \frac{N}{4} G_H(0) \int_y \frac{1}{2}(F_t)^2 + \eta \left[\frac{N^2-1}{2N} \left(G_H(0) - G_H(1) \right) + \frac{N}{4} G_H(1) \right] \cdot \int_y \frac{1}{2} \left(\frac{1}{a} F_z \right)^2$$

$$+ \ldots \tag{3.20}$$

Comparing Eq. (3.20) with Eq. (3.8) we find the following coupling constant renormalizations,

$$\frac{1}{g_t^2} \to \frac{z_{1t}}{g_t^2} = \frac{1}{g_t^2} \cdot \left\{ 1 - g_t^2 \frac{N}{4} G_H(0) \right\}$$

$$\frac{1}{g_s^2} \to \frac{z_{1s}}{g_s^2} = \frac{1}{g_s^2} \cdot \left\{ 1 - g_t^2 \left[\frac{N^2-1}{2N} \left(G_H(0) - G_H(1) \right) + \frac{N}{4} G_H(1) \right] \right\} \tag{3.21}$$

Following Eq. (3.5) and (3.6) we define,

$$\frac{1}{g_H^2} \to \frac{z_{1H}}{g_H^2} \tag{3.22}$$

and note that

$$z_{1H} = \sqrt{z_{1s} z_{1t}} = 1 - g_H^2 \left\{ \frac{N}{4} \sqrt{\eta}\, G_H(0) + \left(\frac{N^2-1}{4N} - \frac{N}{8} \right) \sqrt{\eta} \left(G_H(0) - G_H(1) \right) \right\} \tag{3.23}$$

With these results we have effectively calculated the logarithm of the partition function, $\ln Z_H$, through $O(1)$ and can compare with a similar calculation for the continuum theory using, for instance, a Pauli-Villars regulator mass M,

$$\ln(Z_H/Z) = \frac{z_1}{g^2} \int d^2x \left\{ \frac{1}{2} \sum_\nu (F_\nu)^2 \right\}$$

$$- \frac{z_{1H}}{g_H^2} \left\{ \frac{1}{\sqrt{\eta_R}} \int_y \frac{1}{2}(F_t)^2 + \sqrt{\eta_R} \int_y \frac{1}{2} \left(\frac{1}{a} F_z \right)^2 \right\} \tag{3.24}$$

where we have defined,

$$\eta_R = \eta \frac{z_{1s}}{z_{1t}} = \frac{g_t^2}{g_s^2} \frac{z_{1s}}{z_{1t}} \tag{3.25}$$

Now we take the continuum limit of the Hamiltonian expression $a \to 0$ such that $\eta_R \to 1$ and,

$$\frac{1}{\sqrt{\eta_R}} a \sum \int dt \, \tfrac{1}{2} (\underset{\sim}{F}_t)^2 + \sqrt{\eta_R} \, a \sum \int dt \, \tfrac{1}{2} (\tfrac{1}{a} \underset{\sim}{F}_z)^2 \xrightarrow[a\to 0]{} \int dt \int dz \sum_\nu \tfrac{1}{2} (\underset{\sim}{F}_\nu)^2 \tag{3.26}$$

thus insuring Lorentz invariance of the renormalized theory. The condition $\eta_R \to 1$ as $a \to 0$ is simple to guarantee. Note that if g_s is set to g_t so that $\eta=1$ and the bare theory is Lorentz invariant, then Eq. (3.21) states that the divergent parts of the one loop corrections to z_{1t} and z_{1s} are identical. This implies that $\eta_R = 1$ as $a \to 0$ and the one loop renormalized theory is also Lorentz invariant in the continuum limit. This is clearly an important property of these spin systems. It is also a feature of SU(N) Hamiltonian lattice gauge theory in 3 + 1 dimensions.

Finally, in order to obtain the same physics from the Hamiltonian partition function Z_H and the continuum partition function Z we must require,

$$\frac{z_1}{g^2} = \frac{z_{1H}}{g_H^2} \tag{3.27}$$

or,

$$\frac{1}{Ng^2} - \frac{1}{4} G(0) = \frac{1}{Ng_H^2} - \left\{ \frac{1}{4} \sqrt{\eta}\, G_H(0) + \left(\frac{N^2-1}{4N^2} - \frac{1}{8} \right) \sqrt{\eta} \left(G_H(0) - G_H(1) \right) \right\} \tag{3.28}$$

We introduce the Λ-parameters Λ and Λ_H as discussed in the introduction and write the explicit form for Eq. (1.17)

$$\frac{\Lambda}{aM\Lambda_H} = \exp 2\pi \left[\sqrt{\eta}\, G_H(0) - G(0) \right] \cdot \exp \pi \left[\sqrt{\eta} \left(\frac{2(N^2-1)}{N^2} - 1 \right) \left(G_H(0) - G_H(1) \right) \right] \tag{3.29}$$

$G_H(0)$ and $G_H(1)$ are easily evaluated,

$$\begin{aligned} \sqrt{\eta}\, G_H(0) &= \frac{\sqrt{\eta}}{(2\pi)^2} \int_{-\infty}^{\infty} dk_o \int_{-\pi/a}^{\pi/a} dk \frac{1}{\left[k_o + i \frac{\sqrt{\eta}}{a} \sqrt{4\sin^2(ka/2) + m^2a^2} \right] \left[k_o - i \frac{\sqrt{\eta}}{a} \sqrt{4\sin^2(ka/2) + m^2a^2} \right]} \\ &= \frac{1}{2\pi} \int_{-\pi/a}^{\pi/a} \frac{a\,dk}{2\sqrt{4\sin^2(ka/2) + m^2a^2}} \\ &= \frac{1}{2\pi} \frac{1}{\sqrt{1+m^2a^2/4}} K\left(\frac{1}{1+\frac{m^2a^2}{4}} \right) \end{aligned} \tag{3.30}$$

where K is a complete elliptic integral. Using the asymptotic expansion listed in Appendix A we have,

$$\sqrt{\eta}\, G_H(0) \xrightarrow[m^2a^2\to 0]{} \frac{1}{2\pi} \ln\left(\frac{8}{ma}\right) + O(ma) \tag{3.31}$$

Similarly we calculate,

$$\begin{aligned} \sqrt{\eta} \left(G_H(0) - G_H(1) \right) &= \frac{\sqrt{\eta}}{(2\pi)^2} \int_{-\infty}^{\infty} dk_o \int_{-\pi/a}^{\pi/a} dk \frac{1-\cos ka}{D_H(k)} \\ &= \frac{1}{2\pi} \int_{-\pi/a}^{\pi/a} a\,dk \frac{\sin^2(ka/2)}{\sqrt{4\sin^2(ka/2) + m^2a^2}} \\ &\xrightarrow[m^2a^2\to 0]{} \frac{1}{\pi} \end{aligned} \tag{3.32}$$

Collecting all these results, recalling that $G(0) = \frac{1}{2\pi} \ln(M/m)$, and substituting into Eq. (3.29) we have,

$$\frac{\Lambda}{aM\Lambda_H} = \exp\left[\ln\left(\frac{8}{ma}\right) - \ln\left(\frac{M}{m}\right) \right] \exp\left(\frac{N^2-2}{N^2} \right) \tag{3.33}$$

So,

$$\frac{\Lambda}{\Lambda_H} = 8\ \exp\left(1 - 2/N^2\right) \tag{3.34}$$

A few comments about this result are in order. We observe a large change in scale when passing from the Hamiltonian lattice to the continuum theory. On the other hand, the relation between the Euclidean and Hamiltonian scales follows from Eq. (2.43),

$$\frac{\Lambda_H}{\Lambda_E} = \frac{1}{\sqrt{2}}\ \exp\left[\left(\frac{\pi}{2} - 1\right)\left(1 - 2/N^2\right)\right] \tag{3.35}$$

and this ratio only varies from .94065 ... at N = 2 to 1.2513 ... at $N = \infty$.

We have also calculated Λ/Λ_H for the O(N) vector models by generalizing the Euclidean calculation of ref. (24) to an asymmetric lattice. One finds

$$\left(\frac{\Lambda}{\Lambda_H}\right)_{O(N)} = 8\ \exp\left(\frac{1}{N-2}\right) \tag{3.36}$$

and

$$\left(\frac{\Lambda_H}{\Lambda_E}\right)_{O(N)} = \frac{1}{\sqrt{2}}\ \exp\left[\left(\frac{\pi}{2} - 1\right)\frac{1}{(N-2)}\right] \tag{3.37}$$

Eqs. (3.34), (3.35), (3.36) and (3.37) will be used extensively in later sections of this article.

4. Hamiltonian Lattice Calculations, Continuum Results for the SU(N) x SU(N) Models and Comparisons with O(N) Spin Systems and SU(N) Gauge Theory

We wish to calculate the mass gaps of each of the SU(N) x SU(N) spin systems. This will allow us to obtain each model's β-function for all coupling as well as the numerical relation between each model's scale breaking Λ parameter and the renormalized single particle mass of the continuum limit of the lattice model.

We begin with the Hamiltonian introduced in Sec. 3,

$$H = \frac{\sqrt{\eta}\, g^2}{2a} \sum_{\ell} \left\{ \underset{\sim}{E}^2(\ell) - \frac{2}{g^4}\, \mathrm{tr}\left[U(\ell)U^{+}(\ell+1) + \mathrm{h.c.}\right] \right\} \tag{4.1}$$

where g^2 stands for the g_H^2 of the previous section and $\eta = g_t^2/g_s^2$ as before.

In Eq. (4.1) we take η to be a fixed constant number. This enables us to perform a single-coupling strong coupling analysis in $1/g^2$. The actual value for η is fixed by the requirement that at the matching point onto weak coupling behaviour the renormalized η_R of Eq. (3.25) become equal to one and Lorentz invariance be restored. In the context of a more sophisticated calculational framework one could imagine exploring the g_s-g_t plane for curves which minimize the lattice breaking of Lorentz invariance in the intermediate and strong coupling regions. However, Eq. (4.1) has the advantage that fairly respectable strong coupling series can be developed for it and analyzed in a traditional fashion. Here we shall calculate matrix elements of Eq. (4.1) to $O(g^{-16})$ and match onto known weak coupling, Lorentz invariant perturbation theory to calculate physical quantities.

To calculate the mass gap using strong coupling methods we must calculate the energy of the vacuum and the first excited state(s) of the model and take the difference. At strong coupling ($1/g^4 = 0$) the vacuum must minimize the first term in Eq. (4.1)

$$\underset{\sim}{E}^2(\ell)\ |0\rangle = 0 \tag{4.2}$$

The lowest lying excited states constitute a N^2-fold degenerate subspace. A member of this subspace at zero momentum is described by the wave function

$$|\alpha\beta\rangle = \frac{1}{\sqrt{V}} \sum_m \sqrt{N}\ U_{\alpha\beta}(m)|0\rangle \tag{4.3}$$

Since the quadratic Casimir operator for the fundamental representation of SU(N) is $\frac{N^2-1}{2N}$, the mass gap at strong coupling is,

$$M = \frac{\sqrt{n}Ng^2}{2a} \cdot \frac{(N^2-1)}{2N^2} \qquad (1/g^4 \to 0) \tag{4.4}$$

The higher order corrections to this trivial result are obtained by systematic application of Rayleigh-Schrödinger perturbation theory. All of the ingredients in this calculation are routine and have been illustrated elsewhere except for the SU(N) group theory. The group theory techniques needed to carry out the perturbative calculations can be found in Appendices B and C. The results recorded there are also useful in computations of SU(N) gauge theory. These methods could be extended so that higher orders in the mass gap series could be calculated.

To organize the weak and strong coupling calculations most efficiently one scales the coupling constant g^2,

$$\lambda = g^2 N \tag{4.5}$$

Then the mass gap series have the form,

$$M = \frac{\sqrt{n}\lambda}{2a}\left(\frac{N^2-1}{2N^2}\right)\sum_{m=0}^{\infty} c_m x^m\ , \qquad x = 1/\lambda^2 \tag{4.6}$$

with $c_0 = 1$. Then by direct calculation one finds that the coefficients c_m have finite limits as N is taken to infinity. A proof of this observation can be made most simply using the Euclidean version of the model and following the arguments of ref. 19 for gauge theories rather closely. We have collected the values of c_m for various N in Table 1.

There are several ways of extracting the physics of the continuum limits from these calculations. In one method we choose to renormalize the theory so that M is fixed, independent of a, the lattice spacing. A familiar argument then leads to an expression for the theory's Callan-Symanzik β function,

$$-\frac{\beta(\lambda)}{\lambda} = \frac{\partial \ln \lambda}{\partial \ln a} = \frac{1}{1-2xW'/W} \tag{4.7}$$

where W is the series $\sum c_m x^m$ of Eq. (4.6). Eq. (4.7) will be useful in the strong and intermediate coupling regions. We also can calculate the β function in the weak coupling region. The one loop calculation was done in Sec. 2 and the two loop result is known,[21]

$$-\frac{\beta(\lambda)}{\lambda} = \frac{1}{8\pi}\lambda + \frac{1}{2(8\pi)^2}\lambda^2 + \ldots \tag{4.8}$$

Note that with the definition $\lambda = g^2N$ the second loop of Eq. (4.8) becomes independent of N. This is in sharp contrast with the O(N) models where only the first loop survives the limit. However, it is the same behavior as the SU(N) gauge theories.

One can now plot Eq. (4.7) and (4.8) and see if there is a region in λ where the expressions match. In Fig. (1) we show such a plot for the SU(2) model. There is clear evidence for a match $\lambda \approx 4$ so the curves suggest that the model has a β function whose only zero is at zero coupling. Thus, the continuum limit of the theory is expected to realize the SU(2) x SU(2) symmetry algebraically and possess a non-vanishing renormalized mass gap. Since SU(2) x SU(2) $\approx$ O(4) plots similar to Fig. (1) have appeared in the literature and we note that the low order calculation presented here is in good agreement with the more extensive studies.[6]

In Fig. (2) we present the β functions for N = 2, 6 and infinity. Since our series are rather short we have had to make the assumption that the β functions for all of these models only have zeros at zero coupling. Since the β functions descend very rapidly in the crossover region short series are not capable of describing the match with weak coupling in any detail. However, this working assumption is certainly plausible since the SU(2) x SU(2) model is almost certainly a single phase model and those models with larger N are expected to be more disordered at the same value of λ. Although the details of the strong-weak coupling match for the large N models is not accessible by these calculations the bulk of the crossover region appears to be well-described by our short series. One can check that the higher order terms in the series of Table 1 are small compared to the low order terms throughout the intermediate and strong coupling regions.

It is interesting that the crossover regions of these models become sharper as N increases. Similar behavior has been noted for SU(N) gauge theories in 3+1 dimensions.[5] This phenomenon has led to the suggestion that these lattice regulated models experience the Gross-Witten third order phase transition[13] in the $N \to \infty$ limit, and that at finite N the nearness of those singularities in the complex λ-plane causes the abrupt departure from weak coupling behavior. One can check that the Gross-Witten mechanism occurs in several finite size SU(N)xSU(N) spin systems,[14] so our observation that the systematics of the spin and gauge models are similar seems quite sensible. If we had longer strong coupling series we could follow the path of the singularities in the Padé approximates to the model's β functions as N varies and verify or refute these remarks.

There is one other interesting technical feature in the strong coupling calculation. It is easy to see that the classes of graphs for a particular order of perturbation theory depends on N explicitly. For example, in the SU(3)xSU(3) model the vacuum expectation value for three U matrices is non-vanishing, while in the SU(2)xSU(2) model it is identically zero. The calculations done here to $O(g^{-16})$ required special cases for N= 2,3,4 and 5. Only for $N \geq 6$ does the class of graphs not change with N. Such complications have been noted for gauge theories as well. In addition, not only does one have to include new sets of graphs as one comes down in N, one must also modify some graphs that already existed for large N (large compared to the order of perturbation theory) in order to avoid vanishing energy denominators at small N. These zero energy denominators would appear as singularities in the strong coupling coefficients if one were to naively continue in N. These facts indicate that it is not possible to extrapolate between different SU(N) groups in any simple fashion.

The appearance of special graphs in the $O(g^{-16})$ coefficients for N = 3,4 and 5 render these series rather irregular. This is the reason we have not plotted their β-function in Fig. (2). It has been noted in ref. 26 that such irregularities occur in simple models. However, short series for these models with N sufficiently large do, in fact, well approximate the known exact results. Thus, we believe that our short series results for N = 2 and all $N \geq 6$ are good guides to the real behavior of the SU(N)xSU(N) models. The existence of these complications should be contrasted with a family of models, like the O(N) vector models, which possesses a simple solution in the $N \to \infty$ limit. In these cases the class of graphs for each order of perturbation theory is independent of N, there are no singularities in the strong coupling expansion coefficients for N > 1 and simple 1/N expansions exist. This will be discussed further below.

Next it is interesting to use the asymptotic scaling laws to set the scale of the mass gap calculation. As discussed in Sec. 1 the mass scales of the theory can either be set by studying the deviations from free field behavior in the vicinity of the critical point λ = 0, or by renormalizing the theory holding the mass gap fixed. In a proper renormalized continuum limit these procedures must be related since one mass scale determines all the scales in these models. We can compute the constants C_H relating the gaps M to each theory's Λ_H parameter,

$$M = C_H \Lambda_H \tag{4.9}$$

by plotting the strong coupling calculation for M and fitting it with the weak coupling scaling law for Λ_H

$$\Lambda_H = \frac{1}{a}\sqrt{\frac{8\pi}{\lambda}}\; e^{-8\pi/\lambda}\left[1 + O(\lambda)\right] \tag{4.10}$$

as discussed in Sec. 1. Such plots are shown in Fig. (3) for N = 2,6 and infinity, and the resultant values of C_H are collected in Table 2. To complete this exercise the η parameters of Eq. (4.1) were determined to ensure Lorentz invariance of the lattice models at the matching points of the weak and strong coupling expansions. Recall from section 3 that the one loop renormalization of η was found to be,

$$\eta_R = \eta \cdot \frac{Z_{1s}}{Z_{1t}} = \eta \left\{1 - \frac{\lambda}{\pi}\left[\frac{N^2-1}{2N^2} - \frac{1}{4}\right]\right\} \tag{4.11}$$

and η_R must be fixed at unity so that Lorentz invariance is restored on the lattice of finite lattice spacing and finite bare coupling. The values of λ at the matching can be substituted into Eq. (4.11) and η can be computed. The physical significance of η being different from unity is that the spatial lattice induces a finite calculable renormalization of the speed of light. The effect is not large numerically. For example, $\sqrt{\eta} = 1.08$ for N = 2 and increases to $\sqrt{\eta} = 1.15$ for the $N \to \infty$ limit.

It is particularly interesting to use our calculation of Λ_H/Λ from Sec. 3 and write Eq. (4.9) in the form

$$M = C\Lambda \tag{4.12}$$

because Eq. (4.12) is free of lattice scaffolding--it involves quantities defined in the renormalized continuum limit of these model. The values of C for various N are also listed in Table 2. Eq. (4.12) is this model's analogue of the gauge theory relation between string tension and the scale-breaking parameter of deep inelastic scattering. The error bars in Table 2 reflect our uncertainty in the fits of Fig. (3). It is interesting that the Taylor series for the gaps suffice for the determination of the constants C. If the mass gap series were replaced by Padé approximates our estimates of C change by only a few percent. This stability reflects the fact that at the match between strong and weak coupling expansions in Fig. (3), the higher order strong coupling terms are considerably smaller than the low order terms.

We feel that tabulations of the constants C are a particularly clear way to compare different models. The β functions themselves are only universal near the critical point $\lambda \approx 0$, and the various shapes in Fig. (2) in the intermediate coupling region can be changed by changing the lattice formulation of the model. However, the constants C are invariant to such technicalities--they are properties of the continuum limit and are potentially measurable quantities. A large value of C indicates that non-perturbative effects occur abruptly at a relatively small coupling of a regularized continuum version of the mode. It is interesting that C increases significantly as N increases and that the $N = 6$ results are very close to the $N = \infty$ limit.

We have also carried through this calculational program for the O(N) spin systems. A great deal is known about these models. Their $N \to \infty$ is the soluble mean spherical model whose continuum limit describes a massive, free scalar field. They possess a well-behaved 1/N expansion. Detailed studies of the O(3) model using strong coupling[6] and Monte Carlo Renormalization Group methods[3] have been done. The O(4) model has also been studied

using strong coupling methods to higher orders.[6] The Hamiltonian is,

$$H = \frac{\sqrt{\eta}g}{2a} W = \frac{\sqrt{\eta}g}{2a} \sum_m \left[\underset{\sim}{J}^2(m) - x\, \underset{\sim}{n}(m) \cdot \underset{\sim}{n}(m+1) \right] \tag{4.13}$$

where $\underset{\sim}{J}^2$ is the angular momentum squared in N dimensions and $\underset{\sim}{n}(m)$ is an N-component unit vector on the spatial lattice. The lowest lying excited states of the strong coupling limit of Eq. (4.13) constitute an N-fold degenerate subspace. A member of this subspace at zero momentum is described by the wave function,

$$|\ell\rangle = \frac{1}{\sqrt{V}} \sum_m \sqrt{N}\, n_\ell(m)\, |0\rangle \tag{4.14}$$

where $|0\rangle$ is the strong coupling vacuum,

$$J^2(m)\, |0\rangle = 0 \tag{4.15}$$

appropriate for $N > 1$. To discuss the $N \to \infty$ limit it is convenient to scale the coupling constant,

$$\bar{g} \equiv (N-2)g \quad , \quad y \equiv \frac{2}{\bar{g}^2} = \frac{x}{(N-2)^2} \tag{4.16}$$

Then the mass gap series can be written in the form,

$$M = \frac{\sqrt{\eta}\,\bar{g}}{2a} \left(\frac{N-1}{N-2} \right) \sum_m a_m y_m \tag{4.17}$$

and the coefficients a_m have finite $N \to \infty$ limits. Explicit calculations give the first five coefficients of Eq. (4.16),

$$a_0 = 1$$

$$a_1 = -2 \frac{(N-2)^2}{N(N-1)}$$

$$a_2 = \frac{(N-2)^4}{N^3(N-1)}$$

$$a_3 = \frac{(N-2)^6(2N^2 - \frac{7}{2}N + 3)}{N^5(N-1)^2(N+2)}$$

$$a_4 = -\frac{(N-2)^8(56N^6 - 284N^5 + 55N^4 + 357N^3 - 199N^2 - 67N + 46)}{8N^7(N-1)^3(N+1)(N+2)(2N-1)(2N+1)} \tag{4.18}$$

These coefficients were obtained by extending the O(N) group theory techniques of ref. 30 to handle the product of six spins on a site. The general N calculation was checked against the N = 2,3,4 and mean spherical model results already in the literature. Note that the explicit expressions are well-behaved in the region $N > 1$ where the state Eq. (4.14) lies above the vacuum Eq. (4.14). (Since $J^2 = j(j + N - 2)$, the spin 1 state has greater energy than the spin zero state only for $N > 1$). The β functions for the O(N) models

are obtained from these series as described for the SU(N) x SU(N) models. The resulting curves are shown in Fig. (4). In addition, the constants C_H can be obtained from these fits as described above and using our result for Λ_H/Λ they can be rewritten as results for the more interesting constants C. These results are tabulated in Table 3. Just as in the SU(N) x SU(N) models the values for η in Eq. (4.13) were fixed by requiring that the renormalized η_R be equal to unity at the matching point onto weak coupling behavior. In the O(N) models the one loop renormalization of η is given by,

$$\eta_R = \eta \left\{ 1 - \frac{\bar{g}}{\pi} \cdot \frac{1}{N-2} \right\} \tag{4.19}$$

We learn from Fig. (4) that as N is increased the crossover from weak to strong coupling becomes <u>less</u> abrupt and shifts to <u>larger</u> $\bar{g}$. As a consequence of this the constants C decrease from 3.40 ± .30 for the O(3) model to 1.00 for the $N \to \infty$ limit. Some of these results can be compared with others in the literature. The $N \to \infty$ limit of Eq. (4.13) is soluble[27] and one can determine $\lim_{N\to\infty} C_H = 8$ and $\lim_{N\to\infty} C = 1$ in excellent agreement with our approximate analysis. This is not a new result--it was observed in ref. 27 and 28 that short strong coupling series describe the crossover region of the mean spherical model to good precision. It is more interesting to consider the O(3) model result. A recent Monte Carlo Renormalization Group study[3] of the Euclidean version of the O(3) model determined the correlation length ξ in terms of Λ_E,

$$\xi^{-1} = (100 \pm 30)\ \Lambda_E \tag{4.20}$$

ξ^{-1} is precisely the mass gap of the theory. Since we have calculated Λ_E/Λ 27.212... for N = 3, Eq. (4.19) becomes,

$$M = (3.7 \pm 1.1)\ \Lambda \tag{4.21}$$

in good agreement with our result

$$M = (3.40 \pm .30)\ \Lambda \tag{4.22}$$

These two successes of our calculations suggest that they are quantitative for all N.

And finally, compare these results with SU(N) gauge theories in 3 + 1 dimensions. The Hamiltonian is

$$H = \frac{\sqrt{n}g^2}{2a}\left\{\sum_{\ell} \underset{\sim}{E}_{\ell}^2 - x\sum_{p}\mathrm{tr}\left[U(p) + \mathrm{h.c.}\right]\right\} \quad , \; x = \frac{2}{g^4} \tag{4.23}$$

where $\underset{\sim}{E}_{\ell}^2$ is the quadratic Casimir generator of SU(N) on the link ℓ of a three-dimensional cubic lattice and U(p) is the unitary fundamental representation of the product of group elements on the boundary of a plaquette. As discussed at length elsewhere, the analog of the mass gap of the spin system is the string tension T of the gauge theory. It can be computed by strong coupling methods.

$$T = \frac{\sqrt{n}\lambda}{2a^2}\left(\frac{N^2 - 1}{2N^2}\right)\sum_{m} w_m\left(\frac{1}{\lambda^2}\right)^m \tag{4.24}$$

where $\lambda = g^2N$ is the appropriate coupling constant to discuss the $N \to \infty$ limit since the coefficients w_m then have finite limits.[31] These calculations have been done through $O(\lambda^{-8})$. As in the spin systems, the expansion for T leads to an expansion for the β function by requiring that T be a fixed, physical quantity independent of the lattice spacing. The β function at weak coupling is,

$$-\frac{\beta(\sqrt{\lambda})}{\sqrt{\lambda}} = \frac{11/3}{(16\pi^2)}\lambda + \frac{34/3}{(16\pi^2)^2}\lambda^2 + \dots \tag{4.25}$$

and the Hamiltonian lattice Λ_H parameter is,

$$\Lambda_H = \frac{1}{a}\left(\frac{48\pi^2}{11\lambda}\right)^{51/121} \exp(-24\pi^2/11\lambda)\left[1 + C(\lambda)\right] \tag{4.26}$$

From plots of Eq. (4.24), the derived β function series and Eq. (4.25) we determine the β function curves shown in Fig. (5). Furthermore fits of the string tension series to the asymptotically free scaling law Eq. (4.26) give estimates of the parameters C_H. Using calculations in the literature which relate lattice Λ parameters to continuum quantities we can determine the constants C,

$$\sqrt{T} = C\Lambda_{PV} \tag{4.25}$$

where the subscript P.V. reminds us that the continuum regularization procedure is that of Pauli-Villars. From refs. 23, 25 and 29 we have

$$\Lambda_E/\Lambda_{PV} = .02368 \exp\left(3\pi^2/11N^2\right)$$

$$\Lambda_H/\Lambda_E = .6111 \exp\left[\frac{2\pi^2}{11}\left(\frac{N^2-1}{N^2}\right)\right] \qquad (4.26)$$

The values of C for various N are recorded in Table (4).

Now let us briefly discuss these results. The β functions show the same trends as the SU(N) x SU(N) matrix models. Note, however, that the crossover region is even more abrupt here. The $N \to \infty$ curve goes from the weak coupling match to .9 in about 2.5 units of g^2N while the $N = \infty$ curve of the spin system requires 8.5 units. This difference also shows up in the constants C. They increase with increasing N but their absolute values are considerably larger in the gauge theory in 3 + 1 dimensions than in the spin system in 1 + 1 dimensions.

And finally a word about the theoretical error estimates in Table (4). The SU(3) estimate of C comes from a higher order calculation reported in ref. 2. It was observed there that although short series were adequate to obtain a good β function in the intermediate and strong coupling regions, they were not sufficient to determine C to better than a factor of 2-3. In estimating the values of C for higher N we have assumed that the same systematic trends observed in the SU(3) calculations occur for all N. It is clear from the plots of the β functions that C increases with N but our calculations are not strong enough to give good quantitative estimates. For N = 2 and 3 the results of Table (4) are in good agreement with computer simulations.[1]

Acknowledgments

We thank Drs. D. K. Sinclair and M. Stone for assistance with some of the calculations. J. S. acknowledges useful conversations with Professor A. Jevicki.

Appendix A: Lattice Propagators

We wish to discuss some properties of lattice propagators here. The first is an explicit evaluation of the two dimensional Euclidean square lattice propagator at the origin. We shall find,

$$G(o) = \frac{1}{2\pi}\,\frac{1}{\sqrt{1+\mu^2/4}}\;K\left(\frac{1}{(1+\mu^2/4)^2}\right) \tag{A.1}$$

where K is the complete elliptic integral in the notation of ref.(32) and $\mu^2 = m^2a^2$. In the limit that the infrared mass m is taken to zero, Eq. (A.1) becomes

$$G(o) \sim \frac{1}{4\pi}\ln\left[\frac{32}{m^2a^2}\right] + O(m^2a^2) \tag{A.2}$$

using an asymptotic expansion in ref (32). This result is frequently used in the statistical physics literature. We begin with the definition of the lattice propagator,

$$\left[-\nabla^2+\mu^2\right]G(x) = \sum\left[2G(x) - G(x+\nu) - G(x-\nu)\right] + \mu^2G(x) = \delta_{x,o} \tag{A.3}$$

where the sum runs over the two unit vectors of the square lattice and the right hand side is a kronecker symbol. Introducing the Fourier transform of $G(x)$,

$$G(x) = \int_{-\pi}^{\pi}\frac{dk_1}{2\pi}\int_{-\pi}^{\pi}\frac{dk_2}{2\pi}\;e^{ik.x}\,G(k) \tag{A.4}$$

and substituting into Eq. (A.3) we find

$$G(k) \equiv \frac{1}{\Delta(k)} = (4-2\cos k_1-2\cos k_2+\mu^2)^{-1} \tag{A.5}$$

as used in the text. Note that in Eq. (A.4) we have used the fact that the Brillouin zone corresponding to a square two dimensional lattice is a

square, $-\pi<k_i<\pi, i=1,2$. $G(o)$ can be obtained from Eq. (A.4) by integrating first over k_2 since this is a standard trigonometric integral,

$$G(o) = \frac{1}{2\pi}\int_{-\pi}^{\pi}\frac{dk_1}{\sqrt{\mu^2+4\sin^2(\frac{1}{2}k_1)}\;\sqrt{4+\mu^2+4\sin^2(\frac{1}{2}k_1)}} \tag{A.6}$$

Next change variables to $x = \sin^2(\frac{1}{2}k_1)$,

$$G(o) = \frac{1}{4\pi}\int_{0}^{1}\frac{dx}{\sqrt{x(1-x)\;(\mu^2/4+x)\;(1+\mu^2/4+x)}} \tag{A.7}$$

which is an elliptic integral of the first kind,

$$G(o) = \frac{1}{2\pi}\;\frac{1}{(1+\mu^2/4)}\;F\left(\frac{\pi}{2},\left((1+\mu^2/4)^{-1}\right)\right) \tag{A.8}$$

In the notation of ref. (32), Eq. (A.8) can be written as the more familiar complete elliptic integral K as stated in Eq. (A.1) and the logarithm and the scale of the logarithm in $G(o)$ follow from the asymptotic expansion of K. The fact that $G(o)$ depends logarithmically on μ is clear from Eq.(A.4) and (A.5). It takes considerable care, however, to find the scale in the logarithm - the factor of 32 - and this is the quantity crucial to the discussions of $\Lambda^{P.V.}/\Lambda_L$ given in the text.

Next we need to show that

$$G(1) = \int\frac{d^2k}{(2\pi)^2}\;\frac{e^{ik_1}(e^{-ik_1}-e^{ik_1})}{\Delta^2(k)} \tag{A.9}$$

to complete the derivation of Eq. (2.40). First consider Eq. (A.4) for x=1,

$$G(1) = \int\frac{d^2k}{(2\pi)^2}\;\frac{e^{ik_1}}{\Delta(k)} \tag{A.10}$$

We exponentiate the denominator using the identity

$$\int_0^\infty d\beta\beta^m e^{-\beta\Delta(k)} = \frac{1}{\Delta^{m+1}_{(k)}} \tag{A.11}$$

and find,

$$G(1) = \int_0^\infty d\beta e^{-\beta(4+\mu^2)} \int_0^\pi \frac{dk_1}{\pi} \cos k_1 e^{+2\beta\cos k_1} \int_0^\pi \frac{dk_2}{\pi} e^{+2\beta\cos k_2}$$

$$= \int_0^\infty I_1(2\beta)\, I_o(2\beta) e^{-\beta(4+\mu^2)} d\beta \tag{A.12}$$

where we have identified the k_1 and k_2 integrals as the Besel functions $I_1(2\beta)$ and $I_o(2\beta)$, respectively. Next consider the right hand side of Eq. (A.9),

$$\int \frac{d^2k}{(2\pi)^2} \frac{e^{ik_1}(e^{-ik_1}-e^{ik_1})}{\Delta^2(k)} = 2\int_{-\pi}^{\pi}\frac{dk_1}{2\pi}\int_{-\pi}^{\pi}\frac{dk_2}{2\pi}\frac{\sin^2 k_1}{\Delta^2(k)}$$

$$= 2\int_0^\infty d\beta e^{-\beta(4+\mu^2)}\int_0^\pi \frac{dk_1}{\pi}\beta\sin^2 k_1 e^{2\beta\cos k_1}\int_0^\pi \frac{dk_2}{\pi} e^{2\beta\cos k_2}$$

$$= \int_0^\infty e^{-\beta(4+\mu^2)} I_1(2\beta)\, I_o(2\beta)\, d\beta \tag{A.13}$$

where Eq. (A.11) was used to exponentiate the denominator $\Delta^2(k)$ and the Bessel functions 1/2 $I_1(2\beta)$ and $I_o(2\beta)$ were identified using ref. (32). So Eq. (A.13) is identical with Eq. (A.12) and we are done. It was important to check that the infrared mass μ^2 enters both expression identically.

Appendix B: Quadratic Casimir Operators and Group Weights for General SU(N)

Group theoretical inputs into the strong coupling expansion coefficients include the values $C_2(A)$ of the quadratic Casimir operator for various representations A and so-called group weights $GW(A_1,A_2\cdots)$ which depend on all nontrivial representations $\{A_i\}$ appearing in a given graph. The $C_2(A)$'s appear in the energy denominators and $GW(A_1,A_2\cdots)$ tells us how to weight the contribution from each set of representation $\{A_1,A_2,\cdots\}$. The entire graph will then give,

$$[\text{constant}] \times \sum_{A_1,A_2\cdots} [GW(A_1,A_2\cdots)]\cdot[\text{Function of } C_2(A_1),C_2(A_2)\cdots] \tag{B.1}$$

The [constant] factor depends only on the geometry of the graph (e.g., on the dimension of space time) and not on the symmetry group. In this appendix we show how to calculate $C_2(A)$ and $GW(A_1,A_2\cdots)$ for the group SU(N).

Table B.1 lists low lying representations of SU(N) and some of their properties. The second column labels representations in terms of (N-1) integers $q_i (\geq 0)$, where,

$$q_i = (\text{number of boxes in row } i) - (\text{number of boxes in row } (i+1)) \tag{B.2}$$

Columns 3 and 4 give the dimension of the representation and the value of the quadratic Casimir operator, C_2. A useful formula for the latter quantity can be found for instance in ref. (33)

$$2C_2 = \vec{L}^2 + 2\vec{R}\cdot\vec{L} \tag{B.3}$$

where $\vec{L}$: highest weight vector

$$2\vec{R}: \sum_{\alpha>0} \vec{\alpha} = \text{sum over positive root vectors}$$

(Note that the Casimir operator of ref. (33) differs by a factor of 2 from our C_2.) Given the q_i's one can calculate $\vec{L}$ for any irreducible representation in terms of the (N - 1) so called fundamental weights $\vec{L}^{(i)}$ ($i = 1,2,\ldots N - 1$)

$$\vec{L} = \sum_{i=1}^{N-1} q_i \vec{L}^{(i)} \tag{B.4}$$

$\vec{L}^{(i)}$ and $2\vec{R}$ can be found in the literature (see p. 50 of ref.(33) and p. 299 of ref. (34). For completeness they are reproduced in Table B.2. The components of the vectors in Table B.2 are not all independent and obey,

$$\sum_{1}^{N} \text{components} = 0$$

Given Table B.2 and equations (B.3), (B.4) one can derive the C_2's listed in Table B.1.

We now go on to discuss group weights for the strong coupling diagrams. Recall that the zeroth order vacuum is determined by having all sites in the singlet state. We denote it by

$$|\text{vacuum}\rangle_0 = \prod_{\text{sites}} |0\rangle$$

Excited states are obtained by applying ${}_{\alpha}U_{\beta}^{(\Lambda)}$ on $|\text{vacuum}\rangle_0$ at various sites. We shall label single site states by,

$$|\Lambda;\alpha\beta\rangle = \sqrt{\dim\Lambda}\; {}_{\alpha}U_{\beta}^{(\Lambda)}|0\rangle \tag{B.5}$$

$$\langle\alpha'\beta';\Lambda'|\Lambda;\alpha\beta\rangle = \delta_{\Lambda,\Lambda'}\delta_{\alpha}^{\alpha'}\delta_{\beta'}^{\beta} \tag{B.6}$$

The inner product $\langle\,|\,\rangle$ is defined through the invariant integration over the group $\int dg$ and eq. (B.6) follows from,

$$\int dg\, {}_{\alpha}U_{\beta}^{(\Lambda)}(g)\, {}_{\alpha'}\bar{U}_{\beta'}^{(\Lambda')}(g) = \frac{1}{\dim\Lambda}\delta_{\Lambda,\Lambda'}\delta_{\alpha}^{\alpha'}\delta_{\beta'}^{\beta} \tag{B.7}$$

(We use the notation ${}_{\alpha}\bar{U}_{\beta} \equiv {}_{\beta}U_{\alpha}^{\dagger}$.)

Let

$$f(\Lambda) = \sum_{\alpha,\beta} |\Lambda;\alpha\beta\rangle\langle\alpha\beta;\Lambda| \tag{B.8}$$

be the projection operator onto the subspace spanned by $|\Lambda;\alpha\beta\rangle$ for fixed Λ. We will be interested in calculating the following expectation value at each active site,

$$\langle 0|\, {}_{a_{k+1}}U_{b_{k+1}}^{(\nu_{k+1})} f(\Lambda_k)\, {}_{a_k}U_{b_k}^{(\nu_k)} \cdots\cdots f(\Lambda_2)\, {}_{a_2}U_{b_2}^{(\nu_2)} f(\Lambda_1)\, {}_{a_1}U_{b_1}^{(\nu_1)} |0\rangle$$

$$\equiv P_{a_1a_2\cdots a_{k+1}}(\Lambda_1,\Lambda_2\cdots\Lambda_k)\cdot P^{b_1b_2\cdots b_{k+1}}(\Lambda_1,\Lambda_2\cdots) \tag{B.9}$$

where

ν_i = N or $\bar{N}$ representation

Λ_i = any representation that can appear in the intermediate states

The right hand side of eq. (B.9) introduces the quantities $P_{a_1a_2\ldots}(\Lambda_1,\Lambda_2\cdots)$

which can be regarded as "projection operators" onto the set of representations $\{A_i\}$. Henceforth the term "projection operator" will refer to the P's and not to the f's of eq. (B.8). The latter act on the Hilbert space.

To obtain the group weight $GW(A_1,A_2\cdots)$ for a given strong coupling graph one first writes down the projection operators $P_{a_1a_2\cdots a_{k+1}}(\{A_i\})\cdot P^{b_1b_2\cdots b_{k+1}}(\{A_i\})$ for each active site. Depending on whether $\nu_i = N$ or $\bar{N}$ the indices a_i and b_i must be raised or lowered appropriately. Finally all indices a_i, b_i are contracted out among the active sites in a way dictated by the particular graph. We will give examples of such group weight calculations later in this appendix. Here we first discuss how to obtain the P's.

The unitary representation matrices of SU(N) can be related to each other via the Clebsch-Gordan Series

$$ {}_{a_2}U^{(A_2)}_{b_2}\;{}_{a_1}U^{(A_1)}_{b_1} = \sum_{A,\alpha,\beta} (A_2a_2;A_1a_1\|A\alpha)\,{}_{\alpha}U^{(A)}_{\beta}\,(A\beta\|A_1b_1;A_2b_2) \tag{B.10} $$

where $(A\beta\|A_1b_1;A_2b_2)$ = C-G coefficient and $(A_2a_2;A_1a_1\|A\alpha)$ is obtained from $(A\alpha|A_1a_1;A_2a_2)$ by lowering the upper indices and raising the lower indices. The C-G coefficients obey

$$ \sum_{a_1,a_2} (A'\alpha'\|A_1a_1;A_2a_2)(A_2a_2;A_1a_1\|A\alpha) = \delta^{\alpha}_{\alpha'}\delta_{A,A'} \tag{B.11a} $$

$$ \sum_{\alpha,A} (A\alpha\|A_1a_1';A_2a_2')(A_2a_2;A_1a_1\|A\alpha) = \delta^{a_1'}_{a_1}\delta^{a_2'}_{a_2} \tag{B.11b} $$

Eq. (B.10) can be used repeatedly to obtain,

$$ \langle 0|\,{}_{a_{k+1}}U^{(\nu_{k+1})}_{b_{k+1}}\cdots{}_{a_2}U^{(\nu_2)}_{b_2}\;{}_{a_1}U^{(\nu_1)}_{b_1}|0\rangle = \sum_{A_2,A_3\cdots}\left\{\sum_{\{\alpha_i\}\{\beta_i\}}\left[(\nu_{k+1}a_{k+1};A_k\alpha_k\|0)\left(\prod_{j=3}^{k}(\nu_ja_j;A_{j-1}\alpha_{j-1}|A_j\alpha_j)\right)(\nu_2a_2;\nu_1a_1\|A_2\alpha_2)\right]\left[\begin{matrix} a_i \to b_i \\ \alpha_i \to \beta_i\end{matrix}\right]\right\} $$

Each term in the sum $\sum_{A_2,A_3\cdots}$ corresponds to a projection of the form (B.9). So one sees that

$$ P_{a_1a_2\cdots a_{k+1}}(A_2,A_3,\cdots A_{k-1}) = \sum_{\alpha_2,\alpha_3\cdots}\text{(product of C-G coefficients)} \tag{B.12} $$

(We omit A_1 and A_k since they always refer to the N or $\bar{N}$ representations.)

In practice it is simpler to use C-G series to come in both from the right $\leftarrow|0\rangle$ and from the left $\langle 0|\rightarrow$. Take for example the case k = 3 (4U's)

$$ \begin{aligned} {}_{a_2}U^{(\nu_2)}_{b_2}\;{}_{a_1}U^{(\nu_1)}_{b_1}|0\rangle &= \sum_{A,\alpha,\beta}(\nu_2a_2;\nu_1a_1\|A\alpha)(A\beta\|\nu_1b_1;\nu_2b_2)\,{}_{\alpha}U^{(A)}_{\beta}|0\rangle \\ \langle 0|\,{}_{a_4}U^{(\nu_4)}_{b_4}\;{}_{a_3}U^{(\nu_3)}_{b_3} &= \sum_{A',\alpha',\beta'}(A'\alpha'\|\bar{\nu}_4a_4;\bar{\nu}_3a_3)(\bar{\nu}_3b_3;\bar{\nu}_4b_4\|A'\beta')\langle 0|\,{}_{\alpha'}\bar{U}_{\beta'}(A') \end{aligned} \tag{B.13} $$

Upon using

$$ \langle 0|\,{}_{\alpha'}\bar{U}^{(A)}_{\beta'}\;{}_{\alpha}U^{(A)}_{\beta}|0\rangle = \frac{1}{\dim A}\delta_{A,A'}\delta^{\alpha'}_{\alpha}\delta^{\beta}_{\beta'} \tag{B.14} $$

one finds from (B.13) that

$$ \begin{aligned} P_{a_1a_2a_3a_4}(A) &= \sum_{\alpha}(\nu_2a_2;\nu_1a_1\|A\alpha)\frac{1}{\sqrt{\dim A}}(A\alpha\|\bar{\nu}_4a_4;\bar{\nu}_3a_3) \\ &= \frac{1}{\sqrt{\dim A}}\sum_{\alpha}(\nu_2a_2;\nu_1a_1\|A\alpha)(\nu_3a_3;\nu_4a_4\|\bar{A}\alpha) \end{aligned} \tag{B.15} $$

$$ P^{b_1b_2b_3b_4}(A) = \frac{1}{\sqrt{\dim A}}\sum_{\beta}(A\beta\|\nu_1b_1;\nu_2b_2)(\bar{A}\beta\|\nu_4b_4;\nu_3b_3) $$

In the same way one finds for 6 U's:

$$P_{a_1a_2a_3a_4a_5a_6}(A_2,A_3,A_4) = \frac{1}{\sqrt{\dim A_3}} \sum_{\alpha_2,\alpha_3,\alpha_4} (\nu_2 a_2 : \nu_1 a_1 | A_2\alpha_2)(\nu_3 a_3 : A_2\alpha_2 \| A_3\alpha_3)$$

$$\times (\nu_4 a_4 : \bar{A}_4\alpha_4 \| \bar{A}_3\alpha_3)(\nu_5 a_5 : \nu_6 a_6 \| \bar{A}_4\alpha_4) \qquad (B.16)$$

and a similar expression for $P^{b_1b_2\cdots b_6}(A_2,A_3,A_4)$.

Once one has the C-G coefficients one can calculate the group weights. We mention here that since all the "magnetic indices" a_i and b_i are contracted out one should be able to express the group weight $GW(A_1,A_2\cdots)$ in terms of quantities such as dimA and 6-j symbols that depend only on the representations $(A_1,A_2\cdots)$. In other words one can obtain GW without ever having to make the a_i, b_i dependence in $P_{a_1a_2\cdots}$ explicit. For SU(2) and SU(3) we were indeed able to simplify the GW calculations considerably by using existing tables of 6-j symbols. For general N, however, such tables are not available and one has to go through explicit expressions for the P's.

In the next appendix we derive C-G coefficients for general N. Plugging them into equations (B.15) and (B.16) we arrive at expressions for the P's summarized in tables B.3 and B.4. As one sees a fair amount of notation and definitions had to be introduced to make up these tables. Let us first explain what the symbols mean.

Symmetrization Symbols:

$$\begin{Bmatrix} a_1a_2 \\ b_1b_2 \end{Bmatrix} \equiv \frac{1}{2}\left(\delta^{a_1}_{b_1}\delta^{a_2}_{b_2} + \delta^{a_1}_{b_2}\delta^{a_2}_{b_1}\right)$$

$$\begin{Bmatrix} a_1a_2a_3 \\ b_1b_2b_3 \end{Bmatrix} \equiv \frac{1}{3}\left(\begin{Bmatrix} a_1a_2 \\ b_1b_2 \end{Bmatrix}\delta^{a_3}_{b_3} + \begin{Bmatrix} a_1a_2 \\ b_3b_2 \end{Bmatrix}\delta^{a_3}_{b_1} + \begin{Bmatrix} a_1a_2 \\ b_1b_3 \end{Bmatrix}\delta^{a_3}_{b_2}\right) \qquad (B.17)$$

$\vdots$

With this normalization one has

$$\begin{Bmatrix} a_1a_2 \\ b_1b_2 \end{Bmatrix}\begin{Bmatrix} b_1b_2 \\ c_1c_2 \end{Bmatrix} = \begin{Bmatrix} a_1a_2 \\ c_1c_2 \end{Bmatrix}$$

$$\begin{Bmatrix} a_1a_2a_3 \\ b_1b_2b_3 \end{Bmatrix}\begin{Bmatrix} b_1b_2b_3 \\ c_1c_2c_3 \end{Bmatrix} = \begin{Bmatrix} a_1a_2a_3 \\ c_1c_2c_3 \end{Bmatrix} \qquad (B.18)$$

where all repeated indices are summed from 1 to N, and also

$$\begin{Bmatrix} a_1a_2\cdots a_k \\ a_1a_2\cdots a_k \end{Bmatrix} = \frac{(N-k-1)!}{(N-1)!k!} \qquad (B.19)$$

Antisymmetrization symbols

$$\begin{bmatrix} a_1a_2 \\ b_1b_2 \end{bmatrix} \equiv \frac{1}{2}\left(\delta^{a_1}_{b_1}\delta^{a_2}_{b_2} - \delta^{a_1}_{b_2}\delta^{a_2}_{b_1}\right)$$

$$\begin{bmatrix} a_1a_2a_3 \\ b_1b_2b_3 \end{bmatrix} \equiv \frac{1}{3}\left(\begin{bmatrix} a_1a_2 \\ b_1b_2 \end{bmatrix}\delta^{a_3}_{b_3} - \begin{bmatrix} a_1a_2 \\ b_3b_2 \end{bmatrix}\delta^{a_3}_{b_1} - \begin{bmatrix} a_1a_2 \\ b_1b_3 \end{bmatrix}\delta^{a_3}_{b_2}\right) \qquad (B.20)$$

In general

$$\begin{bmatrix} a_1a_2\cdots a_k \\ b_1b_2\cdots b_k \end{bmatrix} \equiv \frac{1}{(N-k)!k!}\,\varepsilon^{a_1a_2\cdots a_kc_{k+1}\cdots c_N}\varepsilon_{b_1b_2\cdots b_kc_{k+1}\cdots c_N} \qquad (B.21)$$

$$\begin{bmatrix} a_1a_2\cdots a_k \\ a_1a_2\cdots a_k \end{bmatrix} = \frac{N!}{(N-k)!k!} \qquad (B.22)$$

These symbols also obey

$$\begin{bmatrix} a_1a_2 \\ b_1b_2 \end{bmatrix}\begin{bmatrix} b_1b_2 \\ c_1c_2 \end{bmatrix} = \begin{bmatrix} a_1a_2 \\ c_1c_2 \end{bmatrix}$$

$$\begin{bmatrix} a_1a_2 \\ b_1b_2 \end{bmatrix}\begin{Bmatrix} b_1b_2b_3\cdots b_k \\ c_1c_2\cdots\cdots c_k \end{Bmatrix} = 0 \qquad \text{(B.23)}$$

<u>Symbols with mixed upper and lower indices</u>

These are of the form

$$\begin{Bmatrix} a_1a_2\cdots a_k & ; & b_{k+1}\cdots b_p \\ a_{k+1}\cdots a_p & & b_1b_2\cdots b_k \end{Bmatrix} \qquad \text{(B.24)}$$

They are traceless, i.e., they vanish identically when contracted with $\delta^{a_i}_{a_j}$ or $\delta^{b_i}_{b_j}$ ($i \le k$, $j > k$). Examples that we need are:

$$\begin{bmatrix} a_1 & ; & b_2 \\ a_2 & & b_1 \end{bmatrix} \equiv \delta^{a_1}_{b_1}\delta^{b_2}_{a_2} - \frac{1}{N}\,\delta^{a_1}_{a_2}\delta^{b_2}_{b_1} \qquad \text{(B.25)}$$

$$\begin{Bmatrix} a_1 & ; & b_2b_3 \\ a_2a_3 & & b_1 \end{Bmatrix} \equiv \begin{Bmatrix} b_2b_3 \\ a_2a_3 \end{Bmatrix}\delta^{a_1}_{b_1} - \frac{1}{(N+1)}\left(\begin{Bmatrix} a_1b_3 \\ a_2a_3 \end{Bmatrix}\delta^{b_2}_{b_1} + \begin{Bmatrix} b_2a_1 \\ a_2a_3 \end{Bmatrix}\delta^{b_3}_{b_1}\right) \qquad \text{(B.26)}$$

The antisymmetric analogue of (B.26) is

$$\begin{bmatrix} a_1 & ; & b_2b_3 \\ a_2a_3 & & b_1 \end{bmatrix} \equiv \begin{bmatrix} b_2b_3 \\ a_2a_3 \end{bmatrix}\delta^{a_1}_{b_1} - \frac{1}{(N-1)}\left(\begin{bmatrix} a_1b_3 \\ a_2a_3 \end{bmatrix}\delta^{b_2}_{b_1} + \begin{bmatrix} b_2a_1 \\ a_2a_3 \end{bmatrix}\delta^{b_3}_{b_1}\right) \qquad \text{(B.27)}$$

One final object that appears in Table B.4 is

$$\begin{bmatrix} m & ; & b_1b_2\cdots b_{N-2} \\ a_1a_2\cdots a_{N-2} & & n \end{bmatrix} \equiv \begin{bmatrix} b_1b_2\cdots b_{N-2} \\ a_1a_2\cdots a_{N-2} \end{bmatrix}\delta^m_n - \frac{1}{3}\sum_{i=1}^{N-2}\begin{bmatrix} b_1\cdots b_{i-1}\,m\,b_{i+1}\cdots b_{N-2} \\ a_1a_2\cdot\cdot\cdot\cdot\cdot\cdot\cdot a_{N-2} \end{bmatrix}\delta^{b_i}_n \qquad \text{(B.28)}$$

We hope Tables B.3 and B.4 are now a little less mysterious. All repeated dummy variables are summed from 1 to N. Projection operators for other combinations of 4 or 6 U's and/or $\bar{U}$'s can be obtained by appropriately raising and lowering indices. One should also mention that the overall signs of the P's are just a matter of convention. They do not affect the group weights in which the P's are always paired together and appear as $P_{a_1a_2\cdots}(A_2,\cdots) \times P^{b_1b_2\cdots}(A_2,\cdots)$.

Let us now work through a sample group weight calculation. Consider the 4th order graph of Fig. B.1. We label the three active sites 1, 2 and 3 from left to right and follow the time evolution at each site.

<u>site 1</u>:

$$\langle 0|\,{}_{c_1}U^{d_1}\,{}^{a_1}\bar{U}_{b_1}|0\rangle = \frac{1}{N}\,\delta^{a_1}_{c_1}\delta^{d_1}_{b_1} \qquad \text{(B.29)}$$

(eq. (B.29) is a special case of eq. (B.14))

<u>site 3</u>:

$$\langle 0|\,{}_{c_2}U^{d_2}\,{}^{a_2}\bar{U}_{b_2}|0\rangle = \frac{1}{N}\,\delta^{a_2}_{c_2}\delta^{d_2}_{b_2} \qquad \text{(B.30)}$$

<u>site 2</u>:

$$\langle 0|\,{}^{\alpha'}\bar{U}_{\beta'}\,{}^{c_2}\bar{U}_{d_2}\,f(\Lambda_4)\,{}^{c_1}\bar{U}_{d_1}\,f(\Lambda_3)\,{}_{a_2}U^{b_2}\,f(\Lambda_2)\,{}_{a_1}U^{b_1}\,{}_{\alpha}U^{\beta}|0\rangle =$$

$$= P_{\alpha a_1a_2}{}^{c_1c_2\alpha'} \times P^{\beta b_1b_2}{}_{d_1d_2\beta'} \qquad \text{(B.31)}$$

By multiplying (B.29), (B.30) and (B.31) one obtains:

$$\frac{1}{N^2}\left(P_{\alpha a_1a_2}{}^{a_1a_2\alpha'}\right)\left(P^{\beta b_1b_2}{}_{b_1b_2\beta'}\right) \qquad \text{(B.32)}$$

This is to be identified with $GW(\Lambda_2,\Lambda_3,\Lambda_4) \times \frac{1}{N}\,\delta^{\alpha'}_{\alpha}\delta^{\beta}_{\beta'}$, where it is necessary to factor out $\frac{1}{N}\delta^{\alpha'}_{\alpha}\delta^{\beta}_{\beta'}$, to properly take into account the normalization of our one particle state. So

$$\frac{1}{N^2}\left(P_{\alpha a_1 a_2}{}^{a_1 a_2 \alpha'}\right)\left(P^{\beta b_1 b_2}{}_{b_1 b_2 \beta'}\right) \equiv CW(A_2,A_3,A_4)\cdot\frac{1}{N}\,\delta^{\alpha'}_{\alpha}\delta^{\beta}_{\beta'} \tag{B.33}$$

To evaluate the left hand side of (B.33) one looks up the appropriate P's in Table B.4. We must choose the case $(\nu_1,\nu_2,\cdots\nu_6) = (NNN\bar{N}\bar{N}\bar{N})$ and one sees that there are 6 P's to consider.

Take for instance the first P in Table B.4

$$P_{\alpha a_1 a_2}{}^{a_1 a_2 \alpha'} = \sqrt{\frac{6}{N(N+1)(N+2)}}\begin{Bmatrix} a_1 a_2 \alpha' \\ \alpha\, a_1 a_2 \end{Bmatrix} = \sqrt{\frac{(N+2)(N+1)}{6N}}\,\delta^{\alpha'}_{\alpha}$$

Similarly $P^{\beta b_1 b_2}{}_{b_1 b_2 \beta'} = \sqrt{\frac{(N+2)(N+1)}{6N}}\,\delta^{\beta}_{\beta'}$

$$\text{So the left hand side of eq. (B.33)} = \frac{1}{N^2}\frac{(N+2)(N+1)}{6N}\,\delta^{\alpha'}_{\alpha}\delta^{\beta}_{\beta'} \tag{B.35}$$

and one reads off

$$CW(\square\square,\square\square\square,\square\square\square) = \frac{(N+2)(N+1)}{6N^2} \tag{B.36}$$

One can go through similar procedures for the other five possible P's to obtain the results listed in Table B.5.

Appendix C: Clebsch-Gordan Coefficients for General SU(N)

Let ϕ^a and ξ_a $(a = 1,2,\ldots N)$ denote two N dimensional (covariant and contravariant) vectors corresponding to the N and $\bar{N}$ representations of SU(N). In this appendix we consider the cases N>2, so that N and $\bar{N}$ are inequivalent. However, with a few provisos the results are also applicable to the SU(2) case. Irreducible representations can be found by decomposing Kronecker products of ϕ's and ξ's. ϕ and ξ are related by

$$\xi_a = \frac{1}{\sqrt{(N-1)!}}\,\varepsilon_{ab_1b_2\ldots b_{N-1}}\,\phi^{b_1}\phi^{b_2}\ldots\phi^{b_{N-1}} \tag{C.1}$$

In Table C.1 we express the representations already introduced in Table B.1 as tensors built out of ϕ's and ξ's. We use the same symbols defined in eq. (B.17) through (B.28). They can actually be viewed as generalized Kronecker deltas e.g.

$$\delta^{\alpha'}_{\alpha} \rightarrow \delta^{\,a_1'a_2'}_{\,a_1a_2} \equiv \begin{Bmatrix} a_1'a_2' \\ a_1a_2 \end{Bmatrix}. \quad \text{Also} \quad \dim\square\square = \sum_{\alpha=1}^{\dim\square\square}\delta^{\alpha}_{\alpha} \rightarrow \sum_{a_1,a_2=1}^{N}\begin{Bmatrix} a_1a_2 \\ a_1a_2 \end{Bmatrix} = \frac{N(N+1)}{2}$$

A well known example is the decomposition of the product of two ϕ's into a totally symmetric and a totally antisymmetric part.

$$\begin{aligned}
\phi^{a_1}\phi^{a_2} &= \delta^{a_1}_{b_1}\delta^{a_2}_{b_2}\,\phi^{b_1}\phi^{b_2} = \left(\begin{Bmatrix} a_1a_2 \\ b_1b_2 \end{Bmatrix} + \begin{bmatrix} a_1a_2 \\ b_1b_2 \end{bmatrix}\right)\phi^{b_1}\phi^{b_2} \\
&= \left(\begin{Bmatrix} a_1a_2 \\ b_1b_2 \end{Bmatrix}\begin{Bmatrix} b_1b_2 \\ c_1c_2 \end{Bmatrix} + \begin{bmatrix} a_1a_2 \\ b_1b_2 \end{bmatrix}\begin{bmatrix} b_1b_2 \\ c_1c_2 \end{bmatrix}\right)\phi^{c_1}\phi^{c_2} \\
&= \begin{Bmatrix} a_1a_2 \\ c_1c_2 \end{Bmatrix}\left|\square\square^{\{c_1c_2\}}\right\rangle + \begin{bmatrix} a_1a_2 \\ c_1c_2 \end{bmatrix}\left|\begin{smallmatrix}\square\\\square\end{smallmatrix}^{[c_1c_2]}\right\rangle
\end{aligned} \tag{C.2}$$

From eq. (C.2) one reads off the following C-G coefficients

$$\left(\square\square^{\{c_1c_2\}} \,\middle\|\, \square^{a_1}\,;\,\square^{a_2}\right) = \begin{Bmatrix} a_1a_2 \\ c_1c_2\end{Bmatrix} \qquad \text{(C.3)}$$

$$\left(\begin{smallmatrix}\square\\\square\end{smallmatrix}^{[c_1c_2]} \,\middle\|\, \square^{a_1}\,;\,\square^{a_2}\right) = \begin{bmatrix} a_1a_2\\c_1c_2\end{bmatrix}$$

More complicated C-G coefficients can be obtained in the same manner. We give a few more examples

$$\phi^{a_1}\xi_{a_2} = \delta^{a_1}_{b_1}\delta^{b_2}_{a_2}\phi^{b_1}\xi_{b_2} = \left(\begin{bmatrix}a_1 \,;\, b_2\\ a_2 \,;\, b_1\end{bmatrix} + \frac{1}{N}\delta^{a_1}_{a_2}\delta^{b_2}_{b_1}\right)\phi^{b_1}\xi_{b_2}$$

$$= \begin{bmatrix}a_1 \,;\, c_2\\a_2\,;\,c_1\end{bmatrix}\begin{bmatrix}c_1\,;\,b_2\\c_2\,;\,b_1\end{bmatrix}\phi^{b_1}\xi_{b_2} + \frac{1}{\sqrt N}\delta^{\epsilon_1}_{\epsilon_2}\,\frac{1}{\sqrt N}\delta^{b_2}_{b_1}\phi^{b_1}\xi_{b_2}$$

$$= \begin{bmatrix}a_1 \,;\, c_2\\a_2\,;\,c_1\end{bmatrix}\left|\mathrm{Adj}\begin{bmatrix}c_1\\c_2\end{bmatrix}\right> + \frac{1}{\sqrt N}\delta^{\epsilon_1}_{\epsilon_2}\,|1> \qquad \text{(C.4)}$$

Eq. (C.4) leads to

$$\left(\mathrm{Adj}\begin{bmatrix}c_1\\c_2\end{bmatrix}\,\middle\|\,\square^{a_1}\,;\,\overline{\square}_{a_2}\right) = \begin{bmatrix}a_1 \,;\, c_2\\ a_2 \,;\, c_1\end{bmatrix}$$

$$\left(1\,\middle\|\,\square^{a_1}\,;\,\square_{a_2}\right) = \frac{1}{\sqrt N}\delta^{a_1}_{a_2} \qquad \text{(C.5)}$$

Consider a less trivial example

$$\square\square^{\{a_1a_2\}}\xi_{a_3} = \begin{Bmatrix}a_1a_2\\b_1b_2\end{Bmatrix}\delta^{b_3}_{a_3}\phi^{b_1}\phi^{b_2}\xi_{b_3}$$

$$= \left(\begin{Bmatrix}a_1\ a_2 \,;\, b_3\\ a_3 \,;\, b_1\ b_2\end{Bmatrix} + \frac{1}{(N+1)}\begin{Bmatrix}a_1b_3\\b_1b_2\end{Bmatrix}\delta^{a_2}_{a_3} + \frac{1}{(N+1)}\begin{Bmatrix}b_3a_2\\b_1b_2\end{Bmatrix}\delta^{a_1}_{a_3}\right)\phi^{b_1}\phi^{b_2}\xi_{b_3} \qquad \text{(C.6)}$$

The first term gives

$$\left(\begin{smallmatrix}\square&\square\\\vdots&\\\square&\end{smallmatrix}\begin{Bmatrix}c_1\ c_2\\ c_3\end{Bmatrix}\,\middle\|\,\square\square^{\{a_1a_2\}}\,;\,\overline{\square}_{a_3}\right) = \begin{Bmatrix}a_1\ a_2 \,;\, c_3\\ a_3 \,;\, c_1\ c_2\end{Bmatrix} \qquad \text{(C.7)}$$

The last two terms in Eq. (C.6) can be written as (using the symmetry under interchange of a_1 and a_2)

$$\frac{2}{(N+1)}\begin{Bmatrix}a_1\ a_2\\ pq\end{Bmatrix}\begin{Bmatrix}p\ b_3\\b_1b_2\end{Bmatrix}\delta^q_{a_3}\phi^{b_1}\phi^{b_2}\xi_{b_3} = \frac{2}{(N+1)}\begin{Bmatrix}a_1\ a_2\\p\ a_3\end{Bmatrix}\begin{Bmatrix}p\ b_3\\b_1b_2\end{Bmatrix}\phi^{b_1}\phi^{b_2}\xi_{b_3} \qquad \text{(C.8)}$$

One then notes that $\begin{Bmatrix}p\ b_3\\b_1b_2\end{Bmatrix}\phi^{b_1}\phi^{b_2}\xi_{b_3}$ must be proportional to $|\square^p>$. So Eq. (C.8) becomes

$$\frac{2}{(N+1)}\,C\begin{Bmatrix}a_1a_2\\p\ a_3\end{Bmatrix}\,|\square^p>$$

(C = normalization constant)

and

$$\left(\square^p\,\middle\|\,\square\square^{\{a_1a_2\}}\,;\,\overline{\square}_{a_3}\right) = \frac{2C}{N+1}\begin{Bmatrix}a_1a_2\\p\ a_3\end{Bmatrix} \qquad \text{(C.9)}$$

The constant C is fixed by the condition Eq. (B.11a) or

$$\sum_{a_1a_2a_3}\left(\square^p\,\middle\|\,\square\square^{\{a_1a_2\}}\,;\,\overline{\square}_{a_3}\right)\left(\overline{\square}_{a_3}\,;\,\square\square^{\{a_1a_2\}}\,\middle\|\,\square^{p'}\right) = \delta^{p'}_p$$

$$\frac{4C^2}{(N+1)^2}\begin{Bmatrix}a_1a_2\\p\ a_3\end{Bmatrix}\begin{Bmatrix}p'a_3\\a_1a_2\end{Bmatrix} = \frac{4C^2}{(N+1)^2}\begin{Bmatrix}p'a_3\\p\ a_3\end{Bmatrix} = \frac{4C^2}{(N+1)^2}\,\frac{N+1}{2}\,\delta^{p'}_p \equiv \delta^{p'}_p$$

$$\longrightarrow C = \sqrt{\frac{N+1}{2}}$$

So (C.9) becomes

$$\left(\square^p\,\middle\|\,\square\square^{\{a_1a_2\}}\,;\,\overline{\square}_{a_3}\right) = \sqrt{\frac{2}{N+1}}\begin{Bmatrix}a_1a_2\\p\ a_3\end{Bmatrix} . \qquad \text{(C.10)}$$

In Table C.2 we list other C-G coefficients that were obtained in the same way. From them one can construct the projection operators of Table B.3 and B.4 .

References

1. M. Creutz, Phys. Rev. D21 (1980) 2308; Phys. Rev. Lett 45 (1980) 313.
2. K. G. Wilson, Cargèse lectures 1979, Cornell preprint CLNS 80/442.
3. S. Shenker and J. Tobochnik, to be published.
4. J. B. Kogut, R. B. Pearson and J. Shigemitsu, Phys. Rev. Lett. 43 (1979) 484; Illinois preprint ILL-(TH)-80-41, to appear in Phys. Letters. G. Münster, DESY preprint 80/44, May, 1980.
5. J. B. Kogut and J. Shigemitsu, Phys. Rev. Lett. 45 (1980) 410; ibid. 1217 (E).
6. C. Hamer, J. Kogut and L. Susskind, Phys. Rev. Lett. 41 (1978) 1337; Phys. Rev. D19 (1979) 3091. F. Green and S. Samuel, IAS preprint, Dec. 1980.
7. C. Callan, R. Dashen and D. Gross, Phys. Rev. D19 (1979) 1826; Phys. Rev. Lett. 44 (1980) 435.
8. V. A. Fateev, I. V. Frolov and A. S. Schwarz, Nucl. Phys. B154 (1979) 1. B. Berg and M. Lüscher, Comm. Math. Phys. 69 (1979) 57.
9. A. M. Polyakov, Phys. Lett. 82B (1979) 247. Y. Makeenko and A. A. Migdal, Phys. Lett. 88B (1979) 135. A. Jevicki, Brown preprint, HET-441.
10. G. 't Hooft, Nucl. Phys. B72 (1974) 461.
11. J. B. Kogut, J. Shigemitsu and D. K. Sinclair, Illinois preprint, ILL-(TH)-80-52, to appear in Phys. Lett. B.
12. A. A. Migdal, Zk. Eksp. Teor. Fiz. 69, (1975) 810.
13. D. Gross and E. Witten, Phys. Rev. D21 (1980) 446.
14. S. Wadia, Phys. Lett. 93B (1980) 403. D. Friedan, Berkeley preprint, 1980. R. C. Brower, P. Rossi and C. Tan, MIT preprint, 1980, to appear in Phys. Rev. D.
15. A. E. and P. Hasenfratz, CERN preprint TH-2890 (1980). M. Lüscher, G. Münster and P. Weisz, DESY 80/63, to be published in Nucl. Phys. B. C. Itzykson, M. Peskin and J. B. Zuber, Phys. Lett. 95B (1980) 259.

16. J. B. Kogut, R. B. Pearson, J. Richardson, J. Shigemitsu and D. K. Sinclair, Santa Barbara preprint, 1981. See also 2nd entry in ref. 4.
17. B. Lautrup and M. Nauenberg, Copenhagen Conf. on QCD, June 1980.
18. T. H. Berlin and M. Kac, Phys. Rev. 86 (1952) 821. H. E. Stanley, Phys. Rev. 176 (1968) 718.
19. B. DeWit and G. 't Hooft, Phys. Lett. 69B (1977) 61.
20. E. Brezin and J. Zinn-Justin, Phys. Rev. B14 (1976) 3110.
21. A. McKane and M. Stone, Nucl. Phys. B163 (1980) 169.
22. G. 't Hooft, Nucl. Phys. B62 (1973) 444.
23. R. Dashen and D. Gross, Princeton preprint, 1980.
24. G. Parisi, Frascati preprint, 1980.
25. A. Hasenfratz and P. Hasenfratz, Phys. Lett. 93B (1980) 165.
26. H. Neuberger, Berkeley preprint, 1980.
27. M. Srednicki, Phys. Rev. B20 (1979) 3783.
28. J. Banks, Phys. Lett. 93B (1980) 161.
29. D. Gross, Workshop on Lattice Gauge Theory, July 28-August 1, 1980.
30. G. Schelmann, Rockefeller University preprint, 1980; and D. K. Sinclair, private communication.
31. The λ used here differs from that of ref. 5 by a square root.
32. Abramowitz & Stegun, "Handbook of Mathematical Functions," Dover.
33. G. Racah, "Group Theory and Spectroscopy," Ergebnisse der exakten Naturwissenschaften Vol. 37, Springer Verlag.
34. R. Gilmore, "Lie Algebras, and Some of Their Applications," Wiley & Sons, New York, 1974.

Table Captions

1. Expansion coefficients for the mass gap of the SU(N) × SU(N) spin systems.
2. The constants C_H and C for the SU(N) × SU(N) models.
3. Same as Table 2 but for the O(N) spin systems.
4. The constants C for the SU(N) gauge theories. These do not include $\sqrt{n}$ corrections.

.1. Low lying irreducible representations of SU(N).

.2. Fundamental weight vectors of SU(N).

.3. Projection operators for 4 U's (see text for definition of the symbols).

.4. Projection operators for 6 U's.

.5. Group weights for the graph of Fig. B.1.

.1. Tensor notation for the representations of SU(N).

.2. Clebsch-Gordan coefficients for SU(N).

Table 1

N	C_0	C_1	C_2	C_3	C_4
2	1	-21.33333	85.33333	+796.4444	1120.4400
3	1	-9	-139.9500	554.7825	400715.6695
4	1	-8.53333	-7.20593	-15112.8957	4347.6879
5	1	-8.33333	-4.00132	-123.2105	-18302.2934
6	1	-8.22857	-2.58612	-125.9475	-967.9992
8	1	-8.126984	-1.35862	-127.4189	-551.7410
16	1	-8.031373	-.31895	-127.9672	-256.9152
32	1	-8.00782	-.07852	-127.9980	-195.5264
∞	1	-8.0	0.0	-128.0	-176.0

Table 2

N	C_H	C
2	24.14 ± 2.6	1.83 ± .2
6	101.21 ± 2.1	4.92 ± .1
8	115.29 ± 2.1	5.47 ± .1
∞	131.56 ± 2.2	6.05 ± .1

Table 3

N	C_H	C
3	73.95 ± 6.5	3.40 ± .3
4	24.14 ± 2.6	1.83 ± .2
6	13.76	1.34
10	11.33	1.25
∞	8.00	1.00

Table 4

N	C
2	3.71 ± .93
3	6.63 ± 1.44
5	12 - 13
6	13 - 15
30	16 - 18

Table B.1

Young Tableau	$(q_1,q_2\cdots q_{N-1})$	Dimension	Quad. Casimir, C_2
 ≡ fundamental	$(1,0^{N-2})$	N	$\frac{N^2-1}{2N}$
N-1  ≡ 	$(0^{N-2},1)$	N	$\frac{N^2-1}{2N}$
N-1 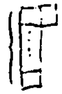 ≡ adjoint	$(1,0^{N-3},1)$	N^2-1	N
	$(2,0^{N-2})$	$\frac{N(N+1)}{2}$	$\frac{(N-1)(N+2)}{N}$
	$(0,1,0^{N-3})$	$\frac{N(N-1)}{2}$	$\frac{(N+1)(N-2)}{N}$
	$(3,0^{N-2})$	$\frac{N(N+1)(N+2)}{6}$	$\frac{3(N-1)(N+3)}{2N}$
	$(1,1,0^{N-3})$	$\frac{N(N^2-1)}{3}$	$\frac{3(N^2-3)}{2N}$
 (for N>2)	$(0,0,1,0^{N-4})$	$\frac{N(N-1)(N-2)}{6}$	$\frac{3(N+1)(N-3)}{2N}$
N-1 	$(2,0^{N-3},1)$	$\frac{N(N+2)(N-1)}{2}$	$\frac{(3N-1)(N+1)}{2N}$
N-1  (for N>2)	$(0,1,0^{N-4},1)$	$\frac{N(N-2)(N+1)}{2}$	$\frac{(3N+1)(N-1)}{2N}$
N-1 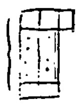 ≡ 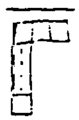	$(1,0^{N-3},2)$	$\frac{N(N+2)(N-1)}{2}$	$\frac{(3N-1)(N+1)}{2N}$
N-2 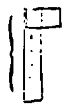 ≡ N-1 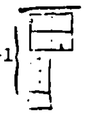 (for N>2)	$(1,0^{N-4},1,0)$	$\frac{N(N-2)(N+1)}{2}$	$\frac{(3N+1)(N-1)}{2N}$

Table B.2

$\vec{L}^{(1)}$: $\frac{1}{N}(N-1, \underbrace{-1, -1, \ldots\ldots, -1}_{(N-1)})$

$\vec{L}^{(2)}$: $\frac{1}{N}(N-2, N-2, -2, -2, \ldots\ldots, -2)$

$\vec{L}^{(3)}$: $\frac{1}{N}(N-3, N-3, N-3, -3, \ldots\ldots, -3)$

$\vdots$

$\vec{L}^{(N-1)}$: $\frac{1}{N}(1, 1, \ldots\ldots 1, -(N-1))$

$2\vec{P}$: $(N-1, N-3, N-5, \ldots, -(N-3), -(N-1))$

Table B.3

$(\nu_1\nu_2\nu_3\nu_4)$	A	$P_{a_1a_2a_3a_4}(A)$
$(N\ \bar{N}\ N\ \bar{N})$		
	singlet ≡ 1	$\frac{1}{N}\delta^{a_2}_{a_1}\delta^{a_4}_{a_3}$
	N-1  ≡ Adj	$\frac{1}{\sqrt{N^2-1}}\left[\begin{matrix} a_2 \\ a_1 \end{matrix} : \begin{matrix} a_4 \\ a_3 \end{matrix}\right]$
$(N\ N\ \bar{N}\ \bar{N})$		
		$\sqrt{\frac{2}{N(N+1)}}\begin{Bmatrix} a_3a_4 \\ a_1a_2 \end{Bmatrix}$
		$\sqrt{\frac{2}{N(N-1)}}\begin{bmatrix} a_3a_4 \\ a_1a_2 \end{bmatrix}$

Table B.4

$(\nu_1\nu_2\nu_3\nu_4\nu_5\nu_6)$	A_2	A_3	A_4	$P_{a_1a_2a_3a_4a_5a_6}(A_2,A_3,A_4)$
$(N\ N\ N\ \bar{N}\ \bar{N}\ \bar{N})$:				
	$\yng(2)$	$\yng(3)$	$\yng(2)$	$\sqrt{\frac{6}{N(N+1)(N+2)}}\begin{Bmatrix} a_4a_5a_6 \\ a_1a_2a_3 \end{Bmatrix}$
	$\yng(1,1)$	$\yng(1,1,1)$	$\yng(1,1)$	$\sqrt{\frac{6}{N(N-1)(N-2)}}\begin{bmatrix} a_4a_5a_6 \\ a_1a_2a_3 \end{bmatrix}$
	$\yng(2)$	$\yng(2,1)$	$\yng(2)$	$\frac{4}{\sqrt{3N(N^2-1)}}\begin{Bmatrix} m & t \\ a_1a_2 \end{Bmatrix}\begin{Bmatrix} a_5a_6 \\ m & q \end{Bmatrix}\begin{bmatrix} q & a_4 \\ t & a_3 \end{bmatrix}$
	$\yng(1,1)$	$\yng(2,1)$	$\yng(1,1)$	$\frac{\sqrt{3}}{\sqrt{N(N^2-1)}}\left(\delta^{a_4}_{a_3}\begin{bmatrix} a_5a_6 \\ a_1a_2 \end{bmatrix} - \begin{bmatrix} a_5a_6a_4 \\ a_1a_2a_3 \end{bmatrix}\right)$
	$\yng(1,1)$	$\yng(2,1)$	$\yng(2)$	$\frac{2}{\sqrt{N(N^2-1)}}\begin{bmatrix} t & a_4 \\ a_1a_2 \end{bmatrix}\begin{Bmatrix} a_5a_6 \\ a_3t \end{Bmatrix}$
	$\yng(2)$	$\yng(2,1)$	$\yng(1,1)$	$\frac{2}{\sqrt{N(N^2-1)}}\begin{Bmatrix} a_4t \\ a_1a_2 \end{Bmatrix}\begin{bmatrix} a_5a_6 \\ t & a_3 \end{bmatrix}$
$(N\ N\ \bar{N}\ N\ \bar{N}\ \bar{N})$:				
	$\yng(2)$	$N-1\left\{\yng(2,1,1)\right.$	$\yng(2)$	$\sqrt{\frac{2}{N(N-1)(N+2)}}\begin{Bmatrix} a_3 & ; & a_5a_6 \\ a_1a_2 & ; & a_4 \end{Bmatrix}$
	$\yng(1,1)$	$N-1\left\{\yng(2,2,1,1)\right.$	$\yng(1,1)$	$\sqrt{\frac{2}{N(N+1)(N-2)}}\begin{bmatrix} a_3 & ; & a_5a_6 \\ a_1a_2 & ; & a_4 \end{bmatrix}$
	$\yng(2)$	$\yng(1)$	$\yng(2)$	$\frac{2}{(N+1)\sqrt{N}}\begin{Bmatrix} t & a_3 \\ a_1a_2 \end{Bmatrix}\begin{Bmatrix} a_5a_6 \\ t & a_4 \end{Bmatrix}$
	$\yng(1,1)$	$\yng(1)$	$\yng(1,1)$	$\frac{2}{(N-1)\sqrt{N}}\begin{bmatrix} t & a_3 \\ a_1a_2 \end{bmatrix}\begin{bmatrix} a_5a_6 \\ t & a_4 \end{bmatrix}$

Table B.4 (cont'd)

$(\nu_1\nu_2\nu_3\nu_4\nu_5\nu_6)$	A_2	A_3	A_4	$P_{a_1a_2a_3a_4a_5a_6}(A_2,A_3,A_4)$
	$\yng(1,1)$	$\yng(1)$	$\yng(2)$	$\frac{2}{\sqrt{N(N^2-1)}}\begin{bmatrix} t & a_3 \\ a_1a_2 \end{bmatrix}\begin{Bmatrix} a_5a_6 \\ t & a_4 \end{Bmatrix}$
	$\yng(2)$	$\yng(1)$	$\yng(1,1)$	$\frac{2}{\sqrt{N(N^2-1)}}\begin{Bmatrix} t & a_3 \\ a_1a_2 \end{Bmatrix}\begin{bmatrix} a_5a_6 \\ t & a_4 \end{bmatrix}$
$(N\ \bar{N}\ \bar{N}\ N\ N\ \bar{N})$:				
	1	$\overline{\yng(1)}$	1	$\frac{1}{N\sqrt{N}}\delta^{a_2}_{a_1}\delta^{a_3}_{a_4}\delta^{a_6}_{a_5}$
	Adj	$\overline{\yng(1)}$	Adj	$\frac{\sqrt{N}}{(N^2-1)}\begin{bmatrix} a_2 & : & a_3 \\ a_1 & : & t \end{bmatrix}\begin{bmatrix} t & : & a_6 \\ a_4 & : & a_5 \end{bmatrix}$
	Adj	$N-2\left\{\yng(2,1,1)\right.$	Adj	$\sqrt{\frac{2}{N(N+1)(N-2)}}\begin{bmatrix} a_2a_3 & : & a_6 \\ a_1 & : & a_4a_5 \end{bmatrix}$
	Adj	$N-1\left\{\yng(3,1,1)\right.$	Adj	$\sqrt{\frac{2}{N(N-1)(N+2)}}\begin{Bmatrix} a_2a_3 & : & a_6 \\ a_1 & : & a_4a_5 \end{Bmatrix}$
	1	$\overline{\yng(1)}$	Adj	$\frac{1}{\sqrt{N(N^2-1)}}\delta^{a_2}_{a_1}\begin{bmatrix} a_3 & : & a_6 \\ a_4 & : & a_5 \end{bmatrix}$
	Adj	$\overline{\yng(1)}$	1	$\frac{1}{\sqrt{N(N^2-1)}}\begin{bmatrix} a_2 & : & a_3 \\ a_1 & : & a_4 \end{bmatrix}\delta^{a_6}_{a_5}$

Table B.4 (cont'd)

$(N\ \bar{\bar{N}}\ N\ N\ \bar{N}\ \bar{N})$:

1				$\frac{1}{N}\sqrt{\frac{2}{N-1}}\,\delta^{a_2}_{a_1}\begin{bmatrix}a_5a_6\\ a_3a_4\end{bmatrix}$
Adj				$\frac{1}{(N-1)}\sqrt{\frac{2}{N+1}}\begin{vmatrix}a_2 & : & t\\ a_1 & & a_3\end{vmatrix}\begin{bmatrix}a_5a_6\\ t\ a_4\end{bmatrix}$
1				$\frac{1}{N}\sqrt{\frac{2}{N+1}}\,\delta^{a_2}_{a_1}\begin{vmatrix}a_5a_6\\ a_3a_4\end{vmatrix}$
Adj				$\frac{1}{(N+1)}\sqrt{\frac{2}{N-1}}\begin{vmatrix}a_2 & : & t\\ a_1 & & a_3\end{vmatrix}\begin{vmatrix}a_5a_6\\ t\ a_4\end{vmatrix}$
Adj	$N-1\{$ 			$\sqrt{\frac{2}{N(N+1)(N-2)}}\begin{bmatrix}a_2 & ; & a_5a_6\\ a_1a_3 & & a_4\end{bmatrix}$
Adj	$N-1\{$ 			$\sqrt{\frac{2}{N(N-1)(N+2)}}\begin{vmatrix}a_2 & ; & a_5a_6\\ a_1a_3 & & a_4\end{vmatrix}$

Table B.5

Λ_2	Λ_3	Λ_4	Group Weight
			$\frac{(N+1)(N+2)}{6N^2}$
			$\frac{(N-1)(N-2)}{6N^2}$
			$\frac{N^2-1}{12N^2}$
			$\frac{N^2-1}{12N^2}$
			$\frac{(N^2-1)}{4N^2}$
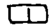			$\frac{(N^2-1)}{4N^2}$

Table C.1

Young Tableau	"Magnetic" Index α	Tensor Representation
$\square$	a	ϕ^a
$\bar{\square}$	a	$\xi_a = \frac{1}{\sqrt{(N-1)!}}\,\epsilon_{ab_1b_2\cdots b_{N-1}}\phi^{b_1}\phi^{b_2}\cdots\phi^{b_{N-1}}$
N-1 $\left\{\begin{smallmatrix}\square\square\\ \vdots\\ \square\end{smallmatrix}\right.$ ≡ Adj	$\begin{bmatrix}a_1\\a_2\end{bmatrix}$	$\begin{bmatrix}a_1 & ; & b_2\\ a_2 & & b_1\end{bmatrix}\phi^{b_1}\xi_{b_2}$
$\square\square$	$\{a_1a_2\}$	$\begin{Bmatrix}a_1a_2\\b_1b_2\end{Bmatrix}\phi^{b_1}\phi^{b_2}$
$\begin{smallmatrix}\square\\\square\end{smallmatrix}$	$[a_1a_2]$	$\begin{bmatrix}a_1a_2\\b_1b_2\end{bmatrix}\phi^{b_1}\phi^{b_2}$
$\square\square\square$	$\{a_1a_2a_3\}$	$\begin{bmatrix}a_1a_2a_3\\b_1b_2b_3\end{bmatrix}\phi^{b_1}\phi^{b_2}\phi^{b_3}$
$\begin{smallmatrix}\square\square\\\square\end{smallmatrix}$	$\begin{bmatrix}m\\a_1a_2\cdots a_{N-2}\end{bmatrix}$	$\begin{bmatrix}m & : & b_1b_2\cdots b_{N-2}\\ a_1a_2\cdots a_{N-2} & & n\end{bmatrix}\phi^n\xi_{b_1}\xi_{b_2}\cdots\xi_{b_{N-2}}$
$\begin{smallmatrix}\square\\\square\\\square\end{smallmatrix}$	$[a_1a_2a_3]$	$\begin{bmatrix}a_1a_2a_3\\b_1b_2b_3\end{bmatrix}\phi^{b_1}\phi^{b_2}\phi^{b_3}$
N-1 $\left\{\begin{smallmatrix}\square\square\square\\ \vdots\\ \square\end{smallmatrix}\right.$	$\begin{Bmatrix}a_1a_2\\a_3\end{Bmatrix}$	$\begin{Bmatrix}a_1a_2 & ; & b_3\\ a_3 & & b_1b_2\end{Bmatrix}\phi^{b_1}\phi^{b_2}\xi_{b_3}$
N-1 $\left\{\begin{smallmatrix}\square\square\\\square\square\\ \vdots\\ \square\end{smallmatrix}\right.$	$\begin{bmatrix}a_1a_2\\a_3\end{bmatrix}$	$\begin{bmatrix}a_1a_2 & ; & b_3\\ a_3 & & b_1b_2\end{bmatrix}\phi^{b_1}\phi^{b_2}\xi_{b_3}$

Table C.2

$$\left(\square\square\ \{b_1b_2\}\ \middle|\ \square^{a_1};\square^{a_2}\right) = \begin{Bmatrix}a_1a_2\\b_1b_2\end{Bmatrix}$$

$$\left(\begin{smallmatrix}\square\\\square\end{smallmatrix}[b_1b_2]\ \middle\|\ \square^{a_1};\square^{a_2}\right) = \begin{bmatrix}a_1a_2\\b_1b_2\end{bmatrix}$$

$$\left(\textcircled{1}\ \middle\|\ \square^{a_1};\bar{\square}_{a_2}\right) = \frac{1}{\sqrt{N}}\,\delta^{a_1}_{a_2}$$

$$\left(\mathrm{Adj}\begin{bmatrix}b_1\\b_2\end{bmatrix}\middle\|\ \square^{a_1};\bar{\square}_{a_2}\right) = \begin{bmatrix}a_1 & ; & b_2\\ a_2 & & b_1\end{bmatrix}$$

$$\left(\square\square\square\ \{b_1b_2b_3\}\ \middle\|\ \square\square^{\{a_1a_2\}};\square^{a_3}\right) = \begin{Bmatrix}a_1a_2a_3\\b_1b_2b_3\end{Bmatrix}$$

$$\left(\begin{smallmatrix}\square\square\\\square\end{smallmatrix}\begin{bmatrix}m\\b_1b_2\cdots b_{N-2}\end{bmatrix}\middle\|\ \square\square^{\{a_1a_2\}};\square^{a_3}\right) = \sqrt{\frac{2}{3}}\,\frac{1}{\sqrt{(N-2)!}}\begin{Bmatrix}a_1a_2\\m\ t\end{Bmatrix}\epsilon^{ta_3b_1b_2\cdots b_{N-2}}$$

$$\left(\begin{smallmatrix}\square\square\\\square\end{smallmatrix}\begin{bmatrix}m\\b_1b_2\cdots b_{N-2}\end{bmatrix}\middle\|\ \begin{smallmatrix}\square\\\square\end{smallmatrix}^{[a_1a_2]};\square^{a_3}\right) = \frac{1}{\sqrt{2}}\,\frac{1}{\sqrt{(N-2)!}}\,\epsilon^{a_1a_2c_1c_2\cdots c_{N-2}}\begin{bmatrix}a_3 & : & b_1b_2\cdots b_{N-2}\\ c_1c_2\cdots c_{N-2} & & m\end{bmatrix}$$

$$\left(\begin{smallmatrix}\square\\\square\\\square\end{smallmatrix}[b_1b_2b_3]\ \middle\|\ \begin{smallmatrix}\square\\\square\end{smallmatrix}^{[a_1a_2]};\square^{a_3}\right) = \begin{bmatrix}a_1a_2a_3\\b_1b_2b_3\end{bmatrix}$$

Table C.2 (cont'd)

$$\left(N-1\left\{\begin{array}{l}\square\square\\ \vdots\\ \square\end{array}\right. \begin{Bmatrix} b_1b_2\\ b_3\end{Bmatrix} \Big\| \ \square\square^{\{a_1a_2\}}\, ; \bar{\square}_{a_3}\right) = \begin{Bmatrix} a_1a_2 & ; & b_3\\ a_3 & & b_1b_2\end{Bmatrix}$$

$$\left(\square^{b} \,\|\, \square\square^{\{a_1a_2\}}\, ; \bar{\square}_{a_3}\right) = \sqrt{\frac{2}{N+1}} \begin{Bmatrix} a_1a_2\\ b\ a_3\end{Bmatrix}$$

$$\left(\square^{b} \,\|\, \begin{array}{c}\square\\ \square\end{array}^{[a_1a_2]}\, ; \bar{\square}_{a_3}\right) = \sqrt{\frac{2}{N-1}} \begin{bmatrix} a_1a_2\\ b\ a_3\end{bmatrix}$$

$$\left(N-2\left\{\begin{array}{l}\square\square\\ \square\square\\ \vdots\\ \square\end{array}\right. \begin{bmatrix} b_1b_2\\ b_3\end{bmatrix} \Big\| \begin{array}{c}\square\\ \square\end{array}^{[a_1a_2]}\, ; \bar{\square}_{a_3}\right) = \begin{bmatrix} a_1a_2 & ; & b_3\\ a_3 & & b_1b_2\end{bmatrix}$$

$$\left(\square^{b} \,\|\, \mathrm{Adj}\begin{bmatrix} a_1\\ a_2\end{bmatrix} ; \square^{a_3}\right) = \sqrt{\frac{N}{N^2-1}} \begin{bmatrix} a_1 & ; & a_3\\ a_2 & & b\end{bmatrix}$$

$$\left(N-1\left\{\begin{array}{l}\square\square\\ \vdots\\ \square\end{array}\right. \begin{Bmatrix} b_1b_2\\ b_3\end{Bmatrix} \Big\| \ \mathrm{Adj}\begin{bmatrix} a_1\\ a_2\end{bmatrix} ; \square^{a_3}\right) = \begin{Bmatrix} a_1a_3 & ; & b_3\\ a_2 & & b_1b_2\end{Bmatrix}$$

$$\left(N-1\left\{\begin{array}{l}\square\square\\ \square\square\\ \vdots\\ \square\end{array}\right. \begin{bmatrix} b_1b_2\\ b_3\end{bmatrix} \Big\| \quad - \text{"} - \qquad \right) = \begin{bmatrix} a_1a_3 & ; & b_3\\ a_2 & & b_1b_2\end{bmatrix}$$

Figure Captions

Fig. 1 β function for the $SU(2) \times SU(2)$ model.

Fig. 2 β functions for the $SU(N) \times SU(N)$ spin systems. The choice of scale. which differs from that of Fig. 1 makes the $SU(2) \times SU(2)$ curve identical to the O(4) model curve of Fig. 4.

Fig. 3 Mass gap fits to asymptotic freedom. The labelled lines are the strong coupling series for $\frac{\sqrt{\lambda}aM}{\sqrt{n}}$ and the straight lines are $\sqrt{\lambda}\ a\Lambda_{H}$ of Eq. (4.10).

Fig. 4 β functions for the O(N) models.

Fig. 5 β functions for SU(N) gauge theories. The λ used here differs from that of ref. 5 by a square root.

Fig. B1 Example of a fourth order diagram. Arrows pointing upwards (downwards) represent $U(\bar{U})$ matrix elements. A_2, A_3 and A_4 stand for representations of SU(N) that can occur in the intermediate states.

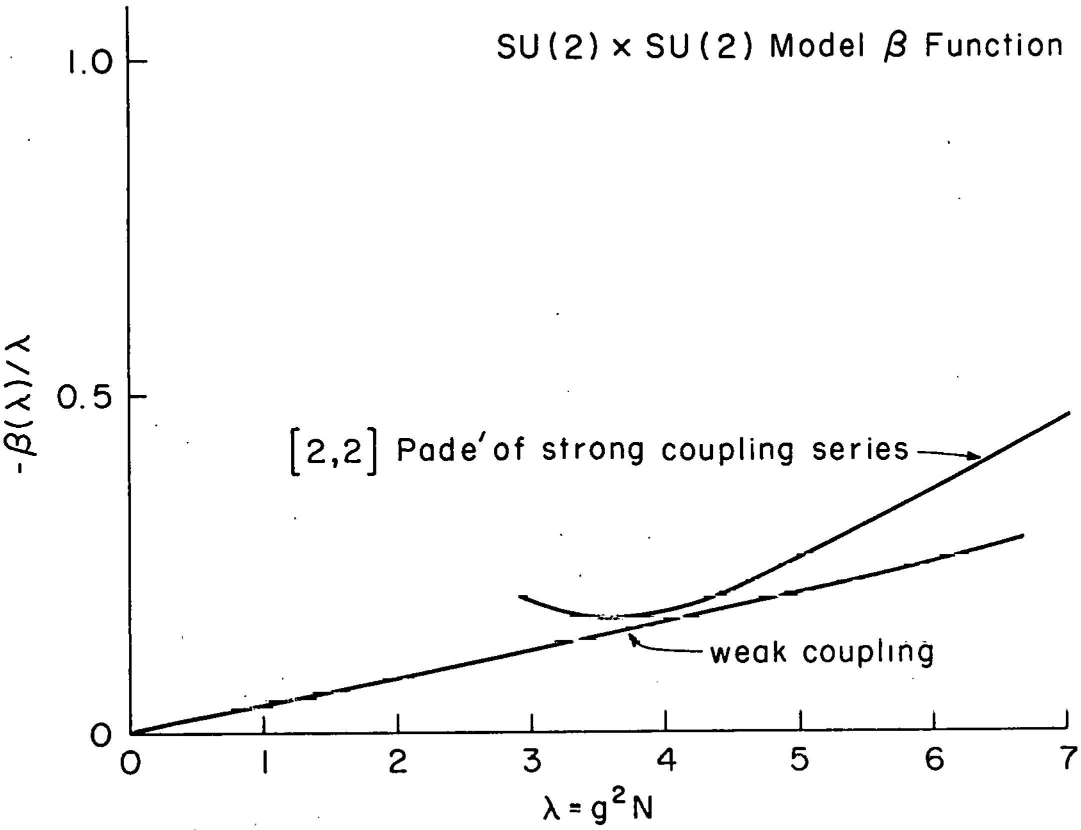
SU(2) × SU(2) Model β Function
1.0
0.5
0
-β(λ)/λ
[2,2] Pade' of strong coupling series
weak coupling
0
1
2
3
4
5
6
7
λ = g² N

Fig. 1

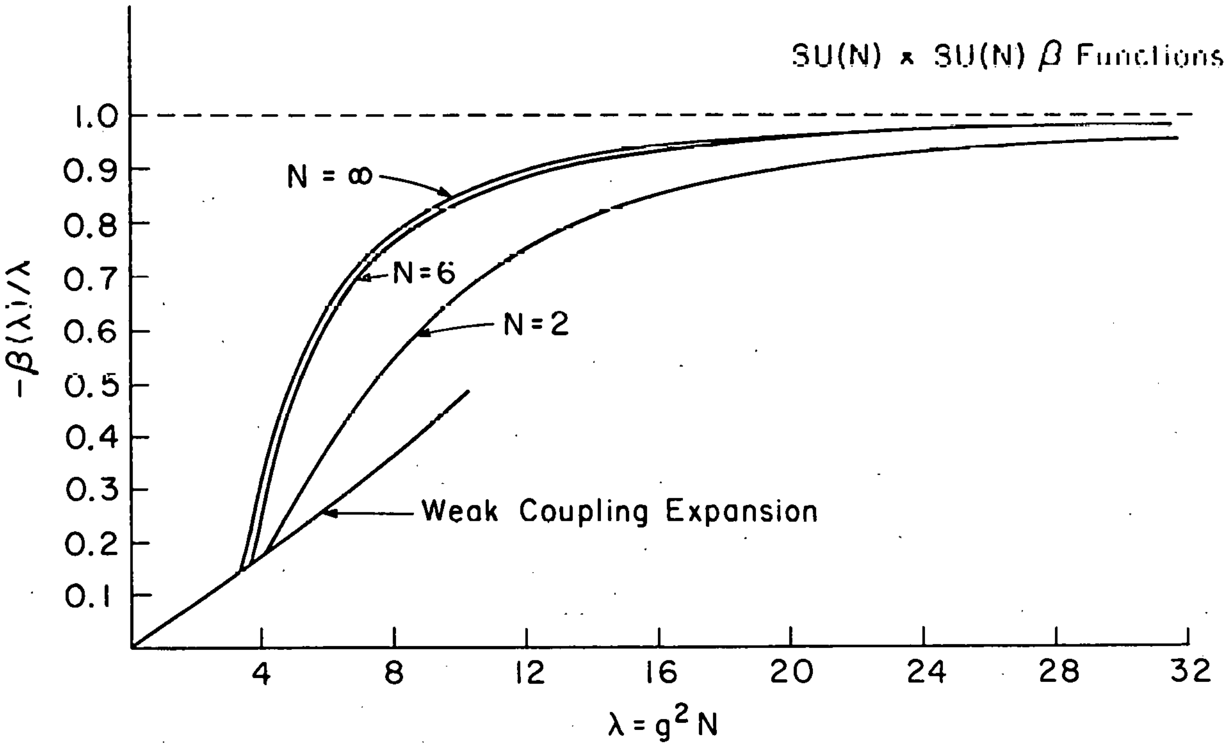
SU(N) × SU(N) β Functions
1.0
0.9
0.8
0.7
0.6
0.5
0.4
0.3
0.2
0.1
-β(λ)/λ
N = ∞
N=6
N=2
Weak Coupling Expansion
4
8
12
16
20
24
28
32
λ = g² N

Fig. 2

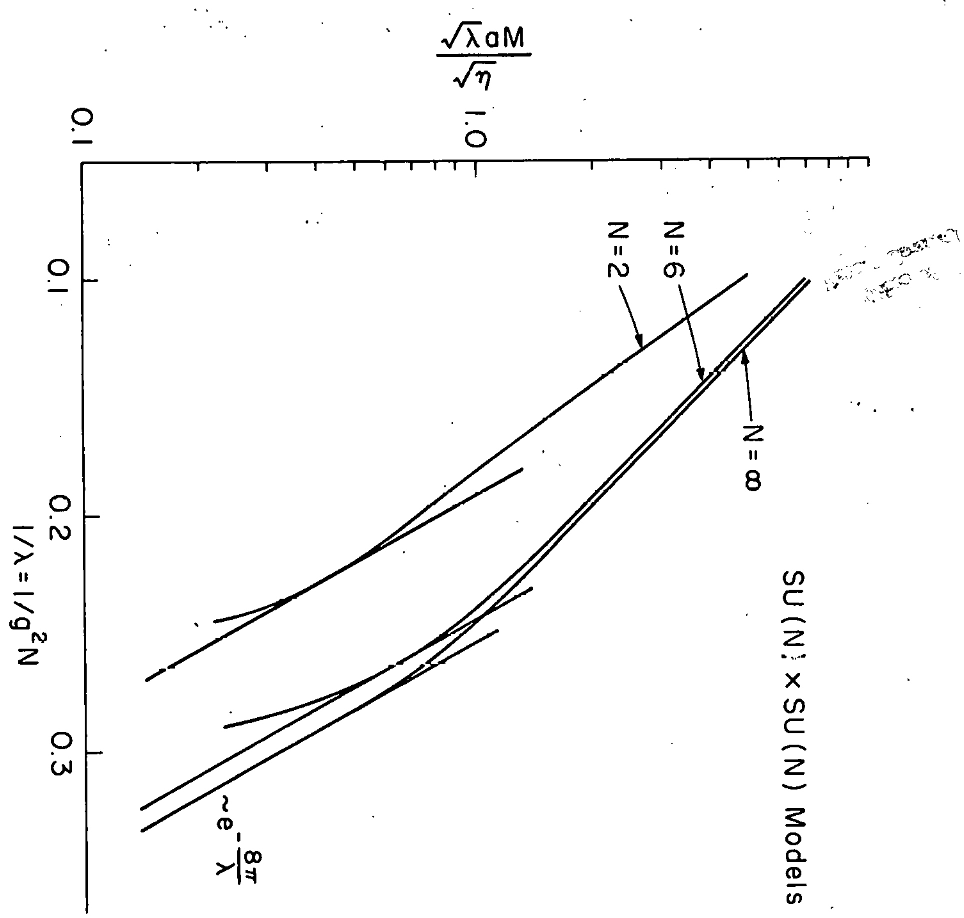
$\frac{\sqrt{\lambda}aM}{\sqrt{\eta}}$
0.1
1.0
N=2
N=6
N=∞
SU(N) × SU(N) Models
$1/\lambda = 1/g^2N$
0.1
0.2
0.3
$\sim e^{-\frac{8\pi}{\lambda}}$

Fig. 3

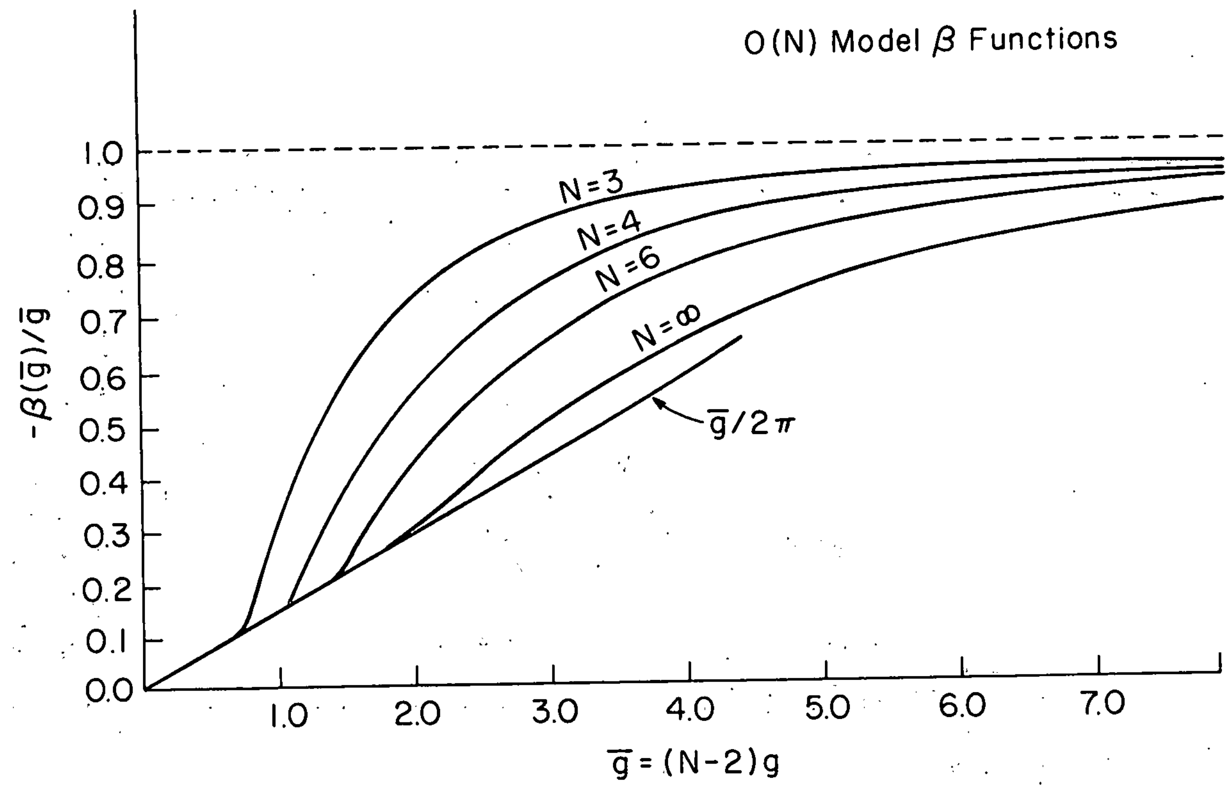
O(N) Model β Functions
1.0
0.9
0.8
0.7
0.6
0.5
0.4
0.3
0.2
0.1
0.0
$-\beta(\overline{g})/\overline{g}$
N=3
N=4
N=6
N=∞
$\overline{g}/2\pi$
1.0
2.0
3.0
4.0
5.0
6.0
7.0
$\overline{g} = (N-2)g$

Fig. 4

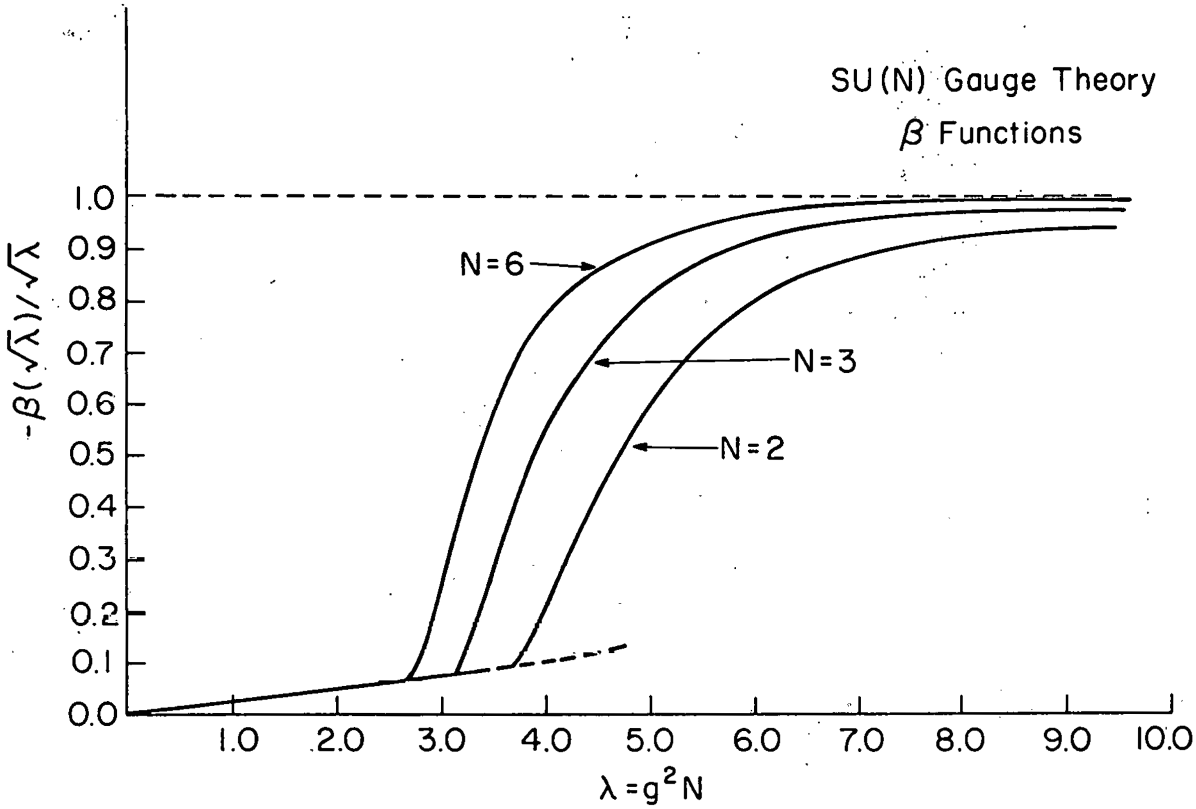
SU(N) Gauge Theory
β Functions
N=6
N=3
N=2
-β(√λ)/√λ
0.0
0.1
0.2
0.3
0.4
0.5
0.6
0.7
0.8
0.9
1.0
2.0
3.0
4.0
5.0
6.0
7.0
8.0
9.0
10.0
λ=g²N

Fig. 5

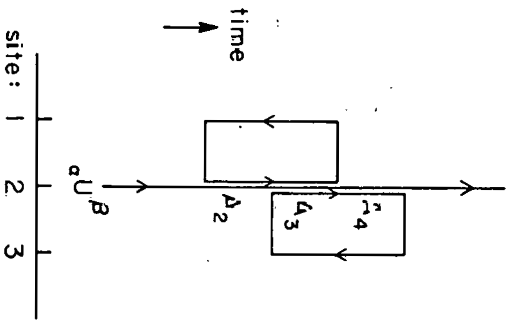
time
site: 1
2
3

Fig. E.1